Chapter 16

# Interactive Effects of Air Pollution and Climate Change on Forest Ecosystems in the United States: Current Understanding and Future Scenarios

Andrzej Bytnerowicz[*,1], Mark Fenn[*], Steven McNulty[†], Fengming Yuan[‡], Afshin Pourmokhtarian[§], Charles Driscoll[§] and Tom Meixner[¶]

[*]*USDA Forest Service, Pacific Southwest Research Station, Riverside, California, USA*

[†]*USDA Forest Service, Southern Station, Raleigh, North Carolina, USA*

[‡]*Climate Change Science Institute and Environmental Science Division, Oak Ridge National Laboratory, Oak Ridge, Tennessee, USA*

[§]*Department of Civil and Environmental Engineering, Syracuse University, Syracuse, New York, USA*

[¶]*University of Arizona, Tucson, Arizona, USA*

[1]*Corresponding author: e-mail: abytnerowicz@fs.fed.us*

**Chapter Outline**



**Developments in Environmental Science, Vol. 13.** http://dx.doi.org/10.1016/B978-0-08-098349-3.00016-5

© 2013 Elsevier Ltd. All rights reserved.

## 16.1 INTRODUCTION

The concepts of air pollution and climate change (CC) are not new. The negative impacts of combustion processes were well known by the thirteenth century (Brimblecombe, 1987), and the atmospheric physics supporting global warming was first postulated in the nineteenth century (Fourier, 1824). While air pollution due to coal and wood combustion is a centuries-old problem, the environmental impacts, including anthropogenic CC and increases in atmospheric carbon dioxide ($CO_2$), that have occurred since the Industrial Revolution, are a comparatively recent field of research (IPCC, 2007). There are strong linkages between CC and air pollution (Jacob and Winner, 2009; Ramanathan and Feng, 2008). While over a dozen gases that contribute to global warming, only a few, such as $CO_2$, methane ($CH_4$), nitrous oxide ($N_2O$), and ozone ($O_3$), make a significant contribution. Carbon dioxide is the major contributor to global warming by trapping heat within the Earth's atmosphere (greenhouse effect) (Solomon et al., 2009). The concentration of $CO_2$ has increased from approximately 270 ppm in the mid-1700s to over 390 ppm today (IPCC, 2007; http://www.esrl.noaa.gov/gmd/ccgg/trends/). Over the past 100 years, the average global surface air temperature has increased by about 0.75 °C in response to the increase in atmospheric greenhouse gases, with approximately 2/3 of that increase occurring since 1980 (IPCC, 2007).

While the scientific community has long recognized the critical need to control atmospheric pollutant emissions, new concerns regarding current and potential future CC impacts emerge. Linkages between CC and air pollution extend to the terrestrial environment, with impacts that are complex and highly variable in time and space. There is a need to investigate the consequences and linkages of the multi-dimensional drivers of global change

effects on ecosystem processes such as current and future CC, air chemistry, atmospheric deposition, and other biotic and abiotic stressors.

Among the environmental pollution factors affecting the growth and health of forests in the United States, ambient ground-level $O_3$ concentrations and atmospheric nitrogen (N) and sulphur (S) deposition are clearly important (Bytnerowicz et al., 2007; Matyssek et al., 2012). Other secondary factors include direct effects of sulphur dioxide ($SO_2$), nitrogen oxides ($NO_x$), fluoride (F) compounds, or trace substances. Consequently, in this chapter, we focus on the interactive effects of $O_3$, N deposition, and changing climate on U.S. forests in the twenty-first century. As examples we present case studies of projections for future changes to forests in the south-western and north-eastern United States under the interactive effects of CC, N deposition, and ambient $O_3$. Due to uncertainties in advances in industrial technologies, energy production and use, and other drivers, projections of future interactive effects of air pollution and CC on U.S. forests have a high degree of imprecision.

## 16.2 AIR POLLUTION, CLIMATE, AND THEIR INTERACTIONS: PRESENT STATUS AND PROJECTIONS FOR THE FUTURE

### 16.2.1 Ozone

$O_3$ is an important greenhouse gas and plays an important role in the radiative budget of the atmosphere through its interactions with both short-wave and long-wave radiation (Gauss et al., 2003). Because $O_3$ is a precursor for oxidizing reactions, it strongly influences the lifetime of such greenhouse gases as methane and hydrofluorocarbons (Gauss et al., 2006). It also indirectly impacts climate by limiting sequestration of $CO_2$ by vegetation (Sitch et al., 2007). Furthermore, the direct radiative effect of $O_3$ provides the third largest positive radiative forcing of the atmospheric greenhouse gases (Gauss et al., 2003). Interestingly, the magnitude of the indirect tropospheric $O_3$ radiative forcing is comparable with its direct radiative effects. Therefore, future reductions in $O_3$ precursor emissions could provide a rapid way to reduce positive anthropogenic radiative forcing in the present atmosphere and may be beneficial in protecting long-term climate safety (Unger and Pan, 2012). Ambient ground-level $O_3$ is an important air pollutant that adversely affects human health and growth and health of forests worldwide (Ainsworth et al., 2012). Increasing worldwide emissions of $O_3$ precursors (i.e. $NO_x$; volatile organic compounds; carbon monoxide, CO) have doubled global background $O_3$ concentrations since the end of the nineteenth century (Brasseur et al., 2001). The current policy-relevant background concentrations in North America (those that would occur without anthropogenic emissions in North America) are $27 \pm 8$ ppb at low-altitude sites and $40 \pm 7$ ppb at high altitude locations as the spring–summer means. The highest values exceeding 60 ppb occur in the intermountain West (McDonald-Buller et al., 2011; Zhang et al., 2011).

Long-range trans-Pacific transport of polluted air masses from Asia is a substantial component of the background $O_3$ in western North America (Vingarzan, 2004). Significant increases of $O_3$ concentrations ($0.63 \pm 0.34$ ppb year$^{-1}$) in the free troposphere have been observed since 1984 during springtime (April–May) when intercontinental transport across the Pacific is most efficient (Cooper et al., 2010; Law, 2010). In addition to the Asian influence, emissions from Canada and Mexico also contribute to background $O_3$ concentrations in the eastern United States and California, respectively (Wang et al., 2009).

A slow but steady decline of peak values of $O_3$ (depicted as the annual fourth highest maximum 8-h averages) for the May–September period has occurred in the United States since 1980. These trends are more pronounced in the eastern than western United States (CASTNET, 2012). Nationwide, the highest $O_3$ pollution occurs in the south-western United States, especially in California where the fourth highest maximum 8-h averages range from 71 to 106 ppb. Moderately elevated $O_3$ levels (fourth highest maximums ranging from 51 ppb in Montana to 78 ppb in New Jersey) occur downwind of urban regions in the rest of the United States (Figure 16.1). The San Bernardino Mountains (SBM) in southern California is the forested area most affected by photochemical smog in the United States (Bytnerowicz et al., 2008); massive dieback of mixed conifer forests occurred there in the 1960s and the 1970s (Arbaugh et al., 1998; Miller et al., 1963). However, between the late 1970s and 2000s, maximum 1-h peak $O_3$ concentrations declined sharply due to implementation of air quality regulations aimed at lowering emissions of $O_3$ precursors. The rate of decline has diminished since 2000,

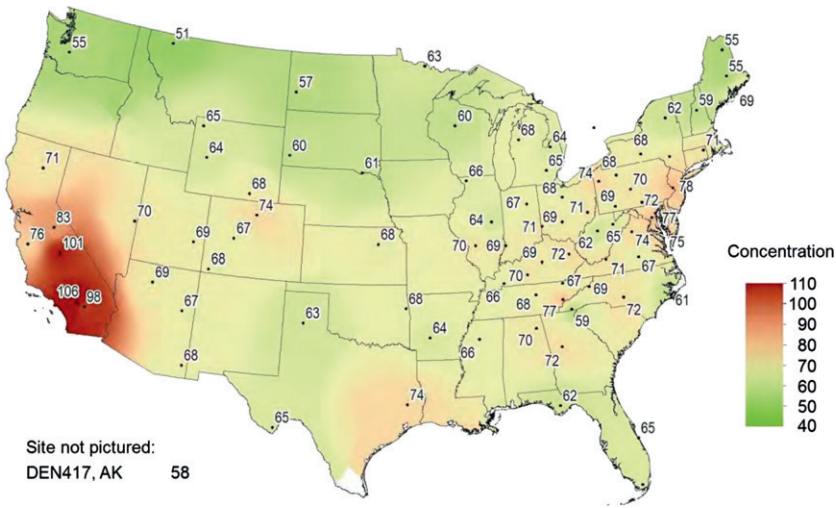


**FIGURE 16.1** Three-year average of fourth highest daily maximum 8-h average ozone concentrations (ppb) for 2008–2010 (CASTNET, 2012).

with maximum hourly values oscillating around 150 ppb and the annual average concentration below 47 ppb. During 1970–2011, $O_3$ concentrations also declined during April–October, the season of greatest vegetative physiological activity. This change was reflected by decreases in AOT40 and W126 indices of more than 50% during this period (Bytnerowicz et al., 2008). These decreases coincide with the recent trends observed in the entire conterminous United States, the western United States, and specifically southern California (Lefohn et al., 2008; Oltmans et al., 2013; Rieder et al., 2013).

Projected changes in anthropogenic emissions are the most important factor in controlling future global and regional $O_3$ concentrations (affecting $O_3$ levels by 40–90%), while changes in natural emissions and climate likely contribute to changes in global $O_3$ levels by 10–30% (Lei et al., 2012). It appears that the risk of hazardous $O_3$ exposure decreases in developed regions such as the United States under the A1B or B1 CC scenarios, while such risks would increase with the A1F1 scenario (Lei et al., 2012). In contrast, however, Doherty et al. (2013) project that at least 20% of precursor emission reductions would be required in some areas to compensate for higher efficiency of $O_3$ photochemical production due to increasing temperatures.

### 16.2.2 Reactive Nitrogen (Nr)

Among Nr species, $NO_x$ results mostly from combustion processes, while ammonia ($NH_3$) and $N_2O$ mostly from agricultural activities. These compounds can affect climate in many different ways. Nitrogen oxides and $NH_3$ contribute to CC indirectly by altering the production and loss of atmospheric CC forcers, both greenhouse gases and aerosols scattering incoming solar radiation. Nitrogen oxides can influence CC by increasing $O_3$ formation (warming effect) and also by increasing removal of $CH_4$ (cooling effect). Additionally, both $NO_x$ and $NH_3$ can enhance light-scattering aerosols (Pinder et al., 2013). Atmospheric concentrations of $NO_x$, nitric acid ($HNO_3$), and particulate nitrate ($NO_3^-$) have decreased significantly since 2003 particularly in the eastern United States largely due to the U.S. Environmental Protection Agency Nitrogen Budget Rule (CASTNET, 2012; NADP, 2010). However, $NH_3$ concentrations and $NH_4^+$ deposition have remained stable, mainly due to a lack of regulatory control of agricultural emissions and excessive use of N fertilizers, the main sources of these compounds (Davidson et al., 2012; Greaver et al., 2012). As for $SO_2$, only local direct phytotoxic effects of reactive N gaseous species occur (Bytnerowicz et al., 1998). Although total atmospheric N deposition has declined due to $NO_x$ emission regulations, it is still elevated in large sections of the eastern United States, in California, and near dispersed urban centres in the western United States (Figure 16.2), and can negatively affect forests and other ecosystems through acidification and eutrophication (Davidson et al., 2012; US EPA, 2008).

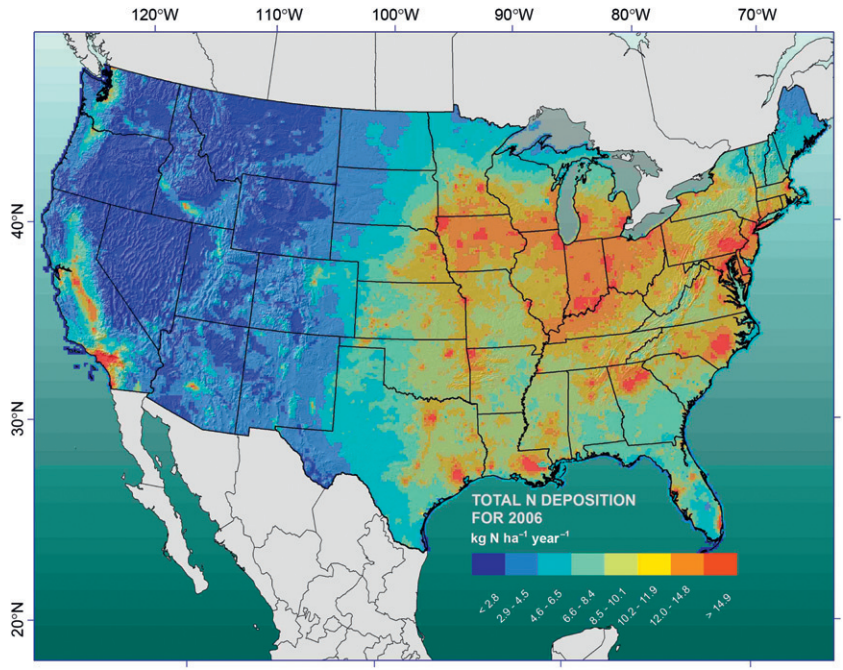


**FIGURE 16.2** Total N deposition in the conterminous United States based on the CMAQ model. *Courtesy of Robin Dennis, EPA and Robert Johnson and Edith Allen, UCR.*

In the eastern United States, broad regions are exposed to moderately elevated N deposition (ca. 8–15 kg N $ha^{-1}$ $year^{-1}$), whereas the western United States is characterized by large areas with N deposition ranging from 3 to 5 kg N $ha^{-1}$ $year^{-1}$ with hotspots and steep deposition gradients found downwind of concentrated agricultural areas or urban, and transportation corridors with deposition as high as 70 kg N $ha^{-1}$ $year^{-1}$. Rapidly expanding regions of energy extraction in the Intermountain West have also led to N deposition hotspots. A key environmental consideration is that many arid, semi-arid, or high elevation ecosystems in the West are characterized by low biomass vegetation that are impacted by N deposition levels as low as 3–6 kg $ha^{-1}$ $year^{-1}$ (Fenn et al., 2003).

Nitrogen deposition also affects greenhouse gas fluxes in terrestrial ecosystems. The net effect of atmospheric N deposition in the United States on long-lived greenhouse gas fluxes currently amounts to an uptake of 170 Tg of $CO_2$ equivalents per year (the result of increased $CO_2$ sequestration and increased emissions of GHGs $CH_4$ and $N_2O$). This net effect is equivalent of 3.2% of the U.S. fossil fuel $CO_2$ emissions and 19% of the total U.S. forestry sector carbon (C) sink (Templer et al., 2012). Approximately 35% of the $CO_2$ emissions from the combustion of fossil fuels in North America are

currently absorbed by terrestrial ecosystems. However, enhanced biogenic emissions of $CH_4$ and $N_2O$ offset at least half of the terrestrial $CO_2$ uptake, and their projected emissions will increase significantly by the end of the twenty-first century (Post and Venterea, 2012).

### 16.2.3 Sulphur Dioxide and Sulphur Deposition

As a result of air quality regulations under the 1970 and 1990 Amendments of the Clean Air Act, $SO_2$ concentrations have been steadily declining since 1973, with decreases of about 40% between 1990 and 2009. Current annual average $SO_2$ values oscillate between 5 and 25 ppb and are well below the national standard of 55 ppb (CASTNET, 2012). Although $SO_2$ still contributes to acidic deposition, its direct phytotoxic effects are limited and only found in small areas in local geographic areas (Legge et al., 1998; US EPA, 2008). Also wet deposition of sulphur (as $SO_4^{2-}$) has significantly decreased in recent decades (Greaver et al., 2012; NADP, 2010).

### 16.2.4 Climate Change Scenarios

Although the impacts of CC on U.S. ecosystems are already being observed, the degree and direction of change is highly variable in time and space (IPCC, 2007). Northern latitudes have generally warmed more than southern latitudes with Alaska, experiencing the largest temperature increase during the twentieth century in the United States (Karl et al., 2009). However, changes in air temperature have been relatively consistent compared to changes in precipitation which have varied over both time and space (Zhang et al., 2007). Over the past 50 years (1958–2008), the south-eastern, south-western, and north-western United States has become 5–40% drier, with the largest reductions occurring in southern California and Arizona (Karl et al., 2009). Conversely, the north-central, south-central, and north-eastern United States has experienced a 10–30% increase in precipitation.

While current levels of CC have impacted U.S. ecosystems, future CC has the potential for major disturbances. Forecasts of future CC involve the use of both alternative models and greenhouse gas emission scenarios. The analyses span the best case (low rates of additional greenhouse gas emissions), and the worst case (high rates of additional greenhouse gas emissions) scenarios. Many factors contribute to these scenarios including demographic and development projections, the rate of emissions from developing countries, and the conversion from fossil fuel to renewable energy resources in developed economies. Various IPCC CC scenarios have been summarized in the Special Report on Emission Scenarios (SRES). Four qualitative storylines have resulted in four sets of scenarios called 'families' A1, A2, B1, and B2 for which six modelling teams developed 40 individual SRES scenarios based on various alternative developments and use of energy technologies (IPCC, 2000).

These scenarios are characterized by a wide range of prediction uncertainties (Stein and Geller, 2012). Using an ensemble of 16 general circulation models (GCMs), Fasullo and Trenberth (2012) recently forecasted that on average, the surface temperature of the Earth will warm by 1.8–4 °C by the end of this century. However, regional warming will vary considerably around this average value.

Given the dynamic nature of CC in both time and space, it is impossible to generalize long-term climatic shifts for any region. However, the pattern of warming is more consistent than the pattern for precipitation change. The most recent U.S. Global Change Research Program Assessment, reported on the Coupled Model Intercomparison Project Three (CMIP3) to provide estimates of future CC across the United States (Karl et al., 2009). By the end of the twenty-first century, all of the United States was projected to warm significantly under all scenarios. Alaska, the Great Plains, and north-central states were predicted to warm the most. Under the low emission scenario, northern Alaska is predicted to warm by 5 °C, while much of the central plain states warm by approximately 3 °C. The least warming was predicted to occur in Florida with 1.5 °C warming by 2100. Warming is already evident by 2050 with the largest increases occurring in the north-central states and Alaska and least warming on the west coast and deep southern states. The high emission scenario exhibits a warming pattern that is similar to the low emission scenario, but the range of air temperature increase is higher (Karl et al., 2009).

Both the amount and timing of precipitation are important factors driving ecosystem impacts. The GCM CMIP3 predicted that under the high emissions scenario, precipitation patterns will have a cyclic nature by the end of the twenty-first century. During the winter, the states south of South Carolina, Kansas, and Utah are predicted to experience significant drying (i.e. 5–25% drier than historical conditions), while more northern states will experience 5–30% more precipitation. As winter turns to spring, the states south of Virginia, Missouri, Wyoming, and Oregon will experience a 5–35% decrease in precipitation compared with historic rates, while in northern states, precipitation will increase by 5–25%. The largest reductions in precipitation are predicted to occur in the already dry areas of southern California. By summer, the drying trend is projected to extend across the entire United States, but moderates to a certain extent with reductions in precipitation ranging from 5% to 40%. Although southern California is not projected to have summer precipitation far below historic values, much of the northwest, central plains, and southern Florida would become the driest areas of the United States. Finally, by autumn, the pattern begins to reverse with spotty patterns (+10% to −10%) of above and below rates of precipitation compared to historic levels. In addition to seasonal changes in precipitation, CMIP3 also projected changes in extreme events (defined as the heaviest 1% of precipitation events). The ensemble GCMs projected that extreme precipitation events

would increase the most in the north-eastern United States (by 67%) and the least (9%) in the south-western United States. Changes in extreme event frequency would likely have significant impacts on flood frequency and other ecosystem disturbances.

It is important to emphasize that the uncertainty of future projections of air pollution and climatic conditions in forests is considerable and forecasts of future effects on ecosystem structure and function are even more uncertain because of complex interactions between various biophysical and climatic factors (Bytnerowicz et al., 2006; McNulty and Boggs, 2010).

## 16.3 PRESENT KNOWLEDGE ON IMPACTS OF AIR POLLUTION, CC, BIOTIC STRESSORS AND MANAGEMENT ON GROWTH AND HEALTH OF FORESTS

Deposition of $O_3$ to terrestrial ecosystems is mostly controlled by stomata (Ainsworth et al., 2012), and a strong correlation between stomatal conductance and potential $O_3$ damage to plants has been established (Reich and Amundson, 1985). Non-stomatal processes are also important and may sometimes dominate total $O_3$ deposition to forests (Kurpius and Goldstein, 2003). High $O_3$ episodes may cause visible foliar injury and affect gas exchange and photosynthesis, resulting in shortened longevity of foliage, reduced plant growth, and impaired health (Grulke et al., 2009). Long-term chronic exposures to $O_3$ can lower stomatal conductance and decrease photosynthesis (Reich and Amundson, 1985). Prolonged exposure to chronic levels of $O_3$ may limit the ability of stomata to close or open rapidly (stomatal sluggishness) (Grulke et al., 2006), increasing water use at the watershed scale (Sun et al., 2012). Short- and long-term reduction of stomatal activity caused by $O_3$ may also reduce the ability of plants to sequester $CO_2$ and is the basis for the indirect $O_3$ greenhouse effect (Sitch et al., 2007). It has been estimated that increased $O_3$ since the Industrial Revolution has decreased photosynthetic $CO_2$ uptake and stomatal conductance of trees by 11% and 13%, respectively (Wittig et al., 2007). Felzer et al. (2004) showed a 2.6–6.8% reduction of annual net primary productivity (NPP) in the conterminous United States in response to $O_3$ levels since 1950 with the largest decreases in the late 1980s and early 1990s. The effects of $O_3$ on loss of C sequestration are similar in magnitude to land use change and offset the increases in C sequestration due to climate warming, $CO_2$, and N fertilization. Simulation of $O_3$ effects on hardwood forests in the north-eastern United States using 1987–1992 $O_3$ data showed declines of annual NPP ranging from 3% to 16% with most pronounced effects at the highest $O_3$ levels and on soils with high water-holding capacity (Ollinger et al., 1997).

Elevated levels of N deposition may have many negative effects, such as changes in biodiversity or contamination of soils and water (Greaver et al., 2012; Pardo et al., 2011; US EPA, 2008). However, moderate amounts of

N from atmospheric deposition have a fertilization effect, stimulating photosynthesis and growth of forest trees and increasing sequestration of $CO_2$ (Davidson et al., 2012). In general, atmospheric N deposition stimulates C sequestration and growth of U.S. forests, although concurrent declines of some tree species, older forests and forests in deposition hotspots occur (Templer et al., 2012). In some highly polluted areas, such as the SBMs of southern California or the Sierra Nevada Mountains, elevated ambient $O_3$ concentrations may offset fertilizing effects of N deposition (Fenn et al., 2003), as documented for ponderosa pine (Peterson et al., 1991).

Ollinger et al. (2002) evaluated separately and in combination the effects of N deposition, surface $O_3$, elevated $CO_2$ and land use history on carbon dynamics of northern U.S. hardwood forests. Their results showed that increases in N deposition and $CO_2$ stimulated forest growth and carbon (C) uptake, but to different degrees following agricultural and timber harvesting. Ambient $O_3$ offset a substantial portion of those increases in those simulations. This decrease in N-induced C sinks by elevated $O_3$ is relevant for much of the global forest lands (as shown above for California forests). Collectively, the combined effects of all factors included in their simulations resulted in growth estimates that were very similar to those obtained in the absence of any form of disturbance. This pattern may suggest that current forests may show little evidence of altered growth since pre-industrial times despite substantial changes in their physical and chemical environment.

Approximately 100 years of effective fire prevention resulted in widespread densification of forest stands, predisposing western forests to drought. Recent climate warming, and, in some areas, the additional effects of $O_3$ and N deposition, have exacerbated drought stress and weakened vast areas of forest making them susceptible to bark beetle attacks. This condition has resulted in large-scale dieback of western U.S. forests. These forests are highly susceptible to catastrophic fires—in 2006 about 4 million hectares burned (Grulke et al., 2009; McKenzie et al., 2009). Comprehensive information on the status of U.S. forests and the health effects of air pollution CC, pests, and diseases has been provided by Tkacz et al. (2008).

## 16.4 POSSIBLE FUTURE CHANGES IN U.S. FORESTS CAUSED BY CLIMATE CHANGE AND AIR POLLUTION

Individually, CC and air pollutants will have various negative (and positive) impacts on ecosystem structure, function and sustainability. Recently, scientists have begun to examine how air pollution may synergistically increase, or antagonistically decrease the impact of CC (McNulty and Boggs, 2010). There are many factors that determine the direction and magnitude of the response. For example, CC may cause an increase in precipitation for a region, which along with the fertilizing impacts of N deposition, may stimulate forest leaf area and growth. Years or decades later, continued CC (or

natural climate variability) may reduce precipitation to sub-historic levels. Unfortunately, forests that have acclimated to a higher precipitation and N regime may have water demands that can no longer be met. These forests may therefore become predisposed to secondary stresses (e.g. insects, disease, wildfire) even though the sites are not in a condition of nitrogen saturation as defined by Aber et al. (2001).

Certain factors associated with CC such as increased air temperatures and changes in precipitation patterns impact forest structure and function as well as its response to atmospheric deposition. Other factors such as tree base cation and N uptake are influenced by growth rates which again are influenced by air temperature and precipitation patterns. Finally, strong acid anion ($SO_4^{2-}$, $NO_3^-$) and base cation leaching are partially controlled by precipitation and air temperature through ecosystem evapotranspiration and soil water outflows. The interaction of these CC factors could significantly alter the capacity of a forest ecosystem to process atmospheric deposition. The north-eastern United States includes considerable forest area that is currently negatively impacted by elevated N and S deposition (McNulty et al., 2007). This region is projected to become both warmer and wetter in the coming decades due to anthropogenic CC (Karl et al., 2009). The trends in CC should positively interact with ecosystem processes that mitigate elevated N and S deposition. Forest productivity and evapotranspiration are both predicted to increase across New England in the coming decades under most CC scenarios (Rustad et al., 2009), which should serve to diminish the effects of acidic deposition. Similarly, negative impacts of acidic deposition could be reduced due to the increased mineral weathering and more available base cations caused by future higher temperatures (Li and McNulty, 2007; Sverdrup and Warfvinge, 1993). However, Wu and Driscoll (2010) observed that critical loads for soil and surface water acidification decreased under future CC scenarios due to increases in leaching losses of $NO_3^-$ associated with higher future temperature. The interactions of CC and atmospheric N deposition, $NO_3^-$ leaching, and acidification in north-eastern forests are discussed in a case study below.

Theoretically, reduced stomatal conductance in response to increasing $CO_2$ levels may enhance plant–water use efficiency, reduce $O_3$ uptake and its potential phytotoxicity (Ainsworth et al., 2012). However, $O_3$-induced damage to stomatal apparatus may confound this effect leading to increased evapotranspiration, reduced stream flow, and increased frequency and severity of drought events as was observed in forest stands in the south-eastern United States over the past 18–26 years (Sun et al., 2012). This example illustrates the complexity of CC–air pollution interactions and the challenges in projecting the effects of combinations of increased temperature, elevated $CO_2$, changing water and nutrient availability, various $O_3$ and N deposition exposure regimes as well as other abiotic and biotic factors. There is a clear need to develop models that integrate multiple biotic and abiotic factors while

projecting future ecosystem changes in order to understand potential risks to forest resources. Such models could provide science-based outcomes and future scenarios and improve our understanding of what adaptive or mitigation measures could be suggested to air resource and land managers.

Below we provide two case studies of simulations of the future impacts of CC, N deposition, and $O_3$ on biomass, nutrient cycling, and water exchange in two forested areas of the United States, southern California, and New England.

## 16.5 PROJECTED HYDROLOGICAL, NUTRITIONAL, AND GROWTH CHANGES IN MIXED CONIFER FORESTS OF THE SBM (SOUTHERN CALIFORNIA) DUE TO CC, N DEPOSITION, AND $O_3$

The DayCent biogeochemistry model (Del Grosso et al., 2000; Parton et al., 1998, 2001), the daily time step version of the CENTURY model (Parton et al., 1993), was modified to include effects of $O_3$ on forests in order to simulate hydrological and biogeochemical (BGC) changes of mixed conifer forests in SBMs under historical and projected CC, N deposition, and $O_3$. Previously DayCent was parameterized for high (Camp Paivika, CP) and low (Barton Flats, BF) N deposition sites (70 and 8.8 kg N $ha^{-1}$ $year^{-1}$, respectively) in the SBM located 70 km east of Los Angeles, California (Fenn et al., 2008). CP is relatively warmer and wetter while BF is cooler and drier (Fenn et al., 2008; Yuan et al., 2011). Arbaugh et al. (1999) applied the CENTURY model to simulate $O_3$ injury in the region using a simple algorithm of halving the rate of foliar turnover from the baseline condition. Here, we introduce an empirical relationship between foliage damage fraction and $O_3$ concentration derived from field data (Grulke and Balduman, 1999), and also a biomass production reduction factor into the DayCent model. The forest biomass production reduction factor is generalized from data in Pye (1988). This reduction factor is a function of the $O_3$ exposure index W126 (Bytnerowicz et al., 2008; Lefohn et al., 1988) because growth decrease was more strongly correlated with $O_3$ dose (concentrations $x$ exposure time) than with $O_3$ exposure concentration alone (Pye, 1988).

The model simulations are driven by historical climate (daily maximal and minimal air temperature, and precipitation) prepared for CP and BF in previous studies (Fenn et al., 2008; Yuan et al., 2011), and extended into 2011. For future conditions (2011–2099), we extracted the NOAA Geophysical Fluid Dynamics Laboratory (GFDL) climate model daily projections of maximal and minimal temperature for two emission scenarios A2 (medium–high emissions) and B1 (low emissions) for both sites (http://cal-adapt.org/data/tabular/; Cayan et al., 2008). Because of some discrepancy between historical observations and GFDL model simulations, adjustments were carried out to match the

model simulations with observations based on the data periods covered by both (Figure 16.3A). For precipitation projections, since the overall changes would be relatively small (less than 10%) (Cayan et al., 2008), we calculated the seasonal air temperature correlation to represent similarity between projection years and historical years and chose the most similar years for assigning the precipitation to a particular projection year. As a result of this approach, the average precipitation (about 880 and 660 mm per year for CP and BF, respectively) did not change from 2011 to 2099, while warming did occur, especially in the medium–high emission scenario A2.

We assumed that $O_3$ concentrations at CP and BF could be represented by two nearby monitoring stations, Crestline (1980–2011) (California Air Resource Board, Air Quality Monitoring Database) and Converse Flat (2004–2010) (CASTNET, 2012) (Figure 16.3B). For the Crestline Station, earlier $O_3$ observations (annual averages) back to 1963 (Bytnerowicz et al., 2008) were combined with hourly $O_3$ monitoring from 1980–2011 to hind cast $O_3$ for the 1940–1963 period assuming that $O_3$ stabilized during the period between the 1950s and early 1960s, and prior to that concentrations increased linearly since 1900 (assuming 10 ppb in 1900; Brasseur et al., 2001). For Converse prior to 2004, seasonal $O_3$ concentration was calculated by a regression of Crestline versus Converse Flat derived from data in Bytnerowicz et al. (2008). At Crestline annual average $O_3$ concentration was slightly lower than at Converse Flat, because higher $O_3$ from June to September at Crestline was offset by lower $O_3$ in the rest of the year (Figure 16.3B and C). We also assumed that the $O_3$ decline since the 1990s would continue until 2099. This decline would bring the current $O_3$ levels back to those prior to 1950 and was denoted as $O_3$ projection treatment 0 ('$O_3$ 0' in Figures 16.4–16.7). In order to capture uncertainty in future projections, the simulations were conducted for four additional $O_3$ projections: $O_3+25\%$, $O_3+50\%$, $O_3-25\%$ and $O_3-50\%$ for $O_3$ levels increased by 25% and 50%, or decreased by 25% and 50% from the '$O_3$ 0'. The $O_3$ projection levels of $O_3+50\%$ would increase $O_3$ up to that in the mid-1970s, while $O_3-50\%$ would decrease $O_3$ level to background by the end of this century. We applied the N deposition datasets for historical simulations in Fenn et al. (2008) in this study and assumed no changes since 2005, that is, 70 kg N $year^{-1}$ at CP and 8.8 kg N $year^{-1}$ at BF, since $O_3$ impacts on forests under CCs were the focus of this study.

Arbaugh et al. (1998) indicates that $O_3$ injury causes foliar biomass loss and higher production and turnover, thus leading to significantly higher litter biomass, but no impact on total tree biomass growth and wood production. In contrast, our simulation showed that as a result of the direct effect of $O_3$ on photosynthesis (reduced productivity) and $O_3$-induced foliar damage, a significant reduction of tree biomass occurred. High levels of $O_3$ exposure are projected to have decreased tree biomass by $\sim$12% at the high N (warm and wet) CP site by the 1980s, with significant decreases occurring since the late 1940s (Figure 16.4C). The decrease in tree biomass was much less pronounced

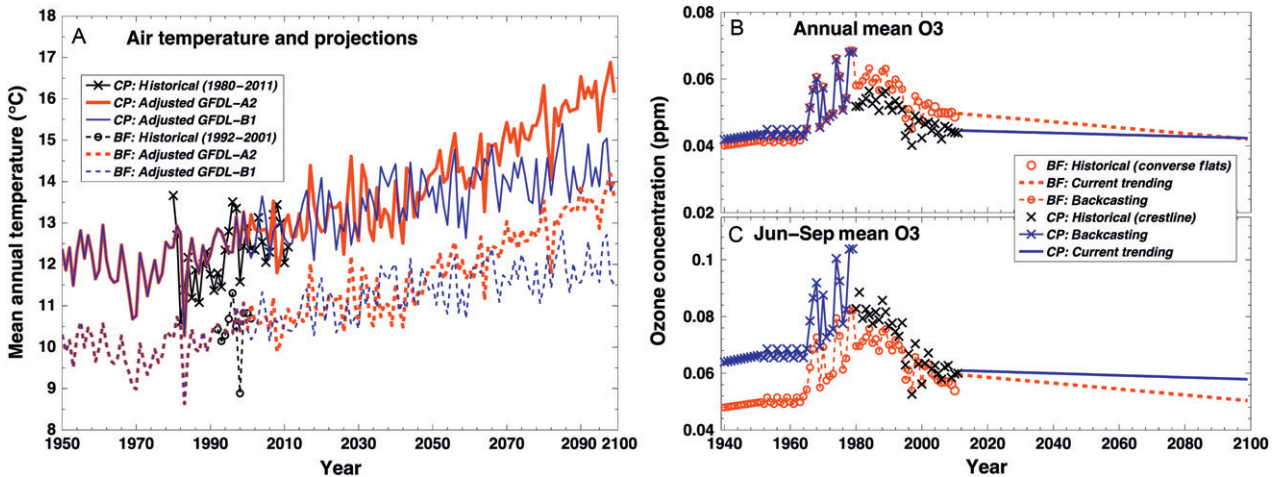


**FIGURE 16.3** Historical and projected climate and ozone trends at Camp Paivika (CP, high N deposition of 70 kg N $year^{-1}$) and Barton Flat (BF, low N deposition of 8.8 kg N $year^{-1}$) in SBM to drive DAYCENT model: (A) air temperature and adjusted GFDL projections (emission scenario A2 (medium–high emissions) and B1 (low emissions)), (B) Annual mean $O_3$ concentrations and its trending, and (C) June–September mean $O_3$ concentrations and its trending.

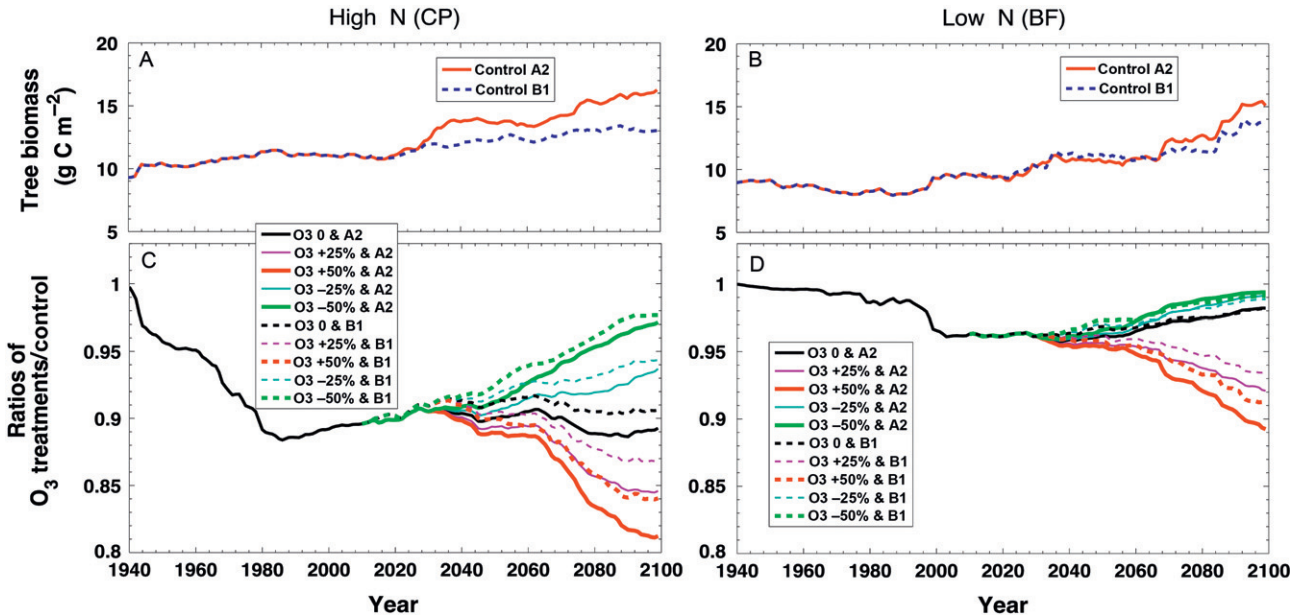


**FIGURE 16.4** Reduction of forest tree biomass caused by $O_3$ under different CC and N deposition scenarios in SBM. Note that A2 and B1 stands for GFDL projections with Scenario A2 and B1; Treatment '$O_3$ 0' is historical $O_3$ concentration and current trending is extended until 2099 (see Figure 16.3B and C), and $O_3 + 25\%$, $+50\%$, $-25\%$, and $-50\%$ are $O_3$ concentration changes of $+25\%$, $+50\%$, $-25\%$, and $-50\%$ of the '$O_3$ 0' treatment; control is a simulation without $O_3$ effects.

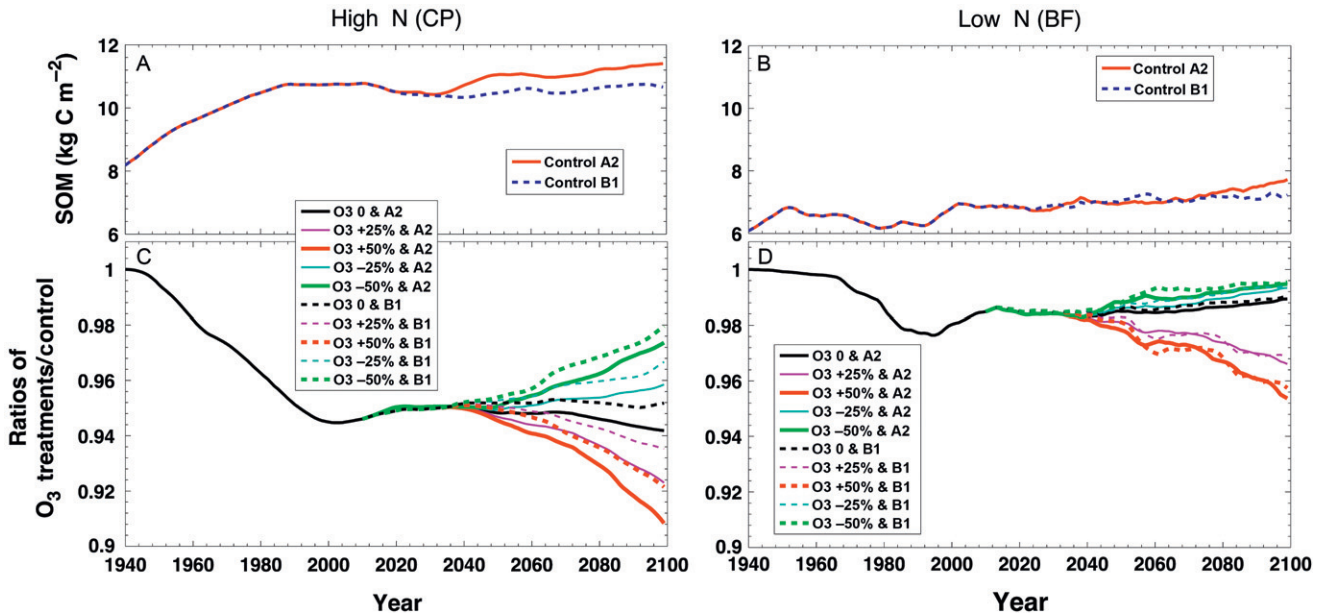


**FIGURE 16.5** Reduction of forest soil organic matter (SOM) caused by $O_3$ under different CC and N deposition scenarios in SBM. See Figure 16.4 for details of the treatments.

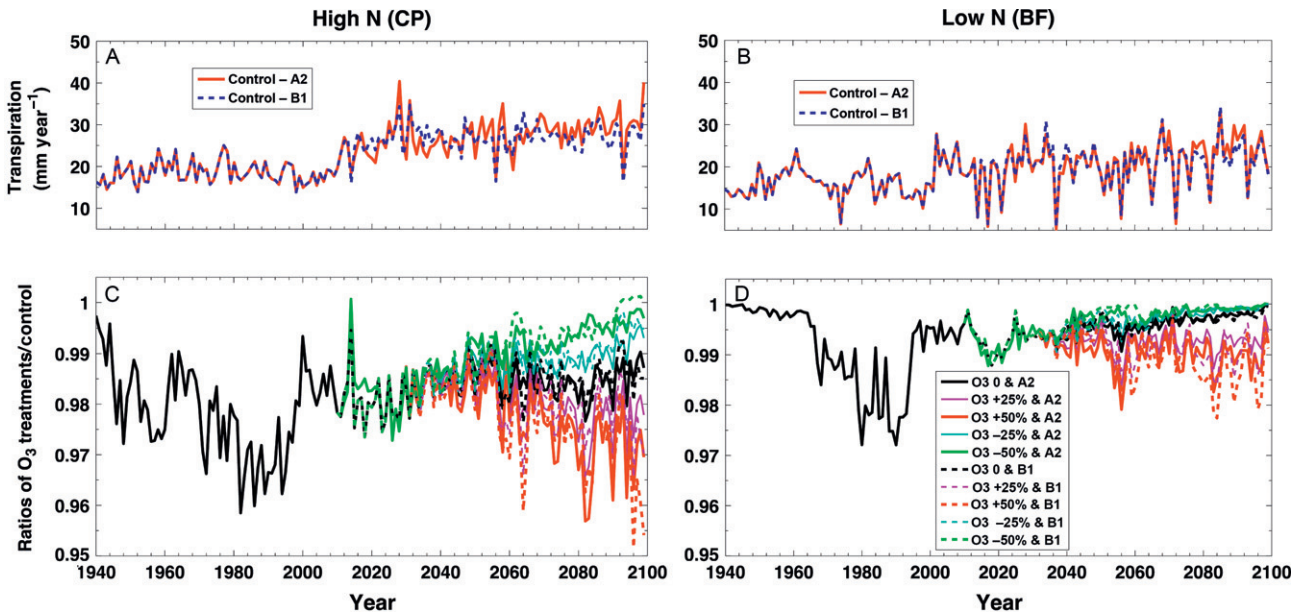


**FIGURE 16.6** DAYCENT simulated plant transpiration under CC and N deposition and $O_3$ effects in SBM. See Figure 16.4 for details of the treatments.

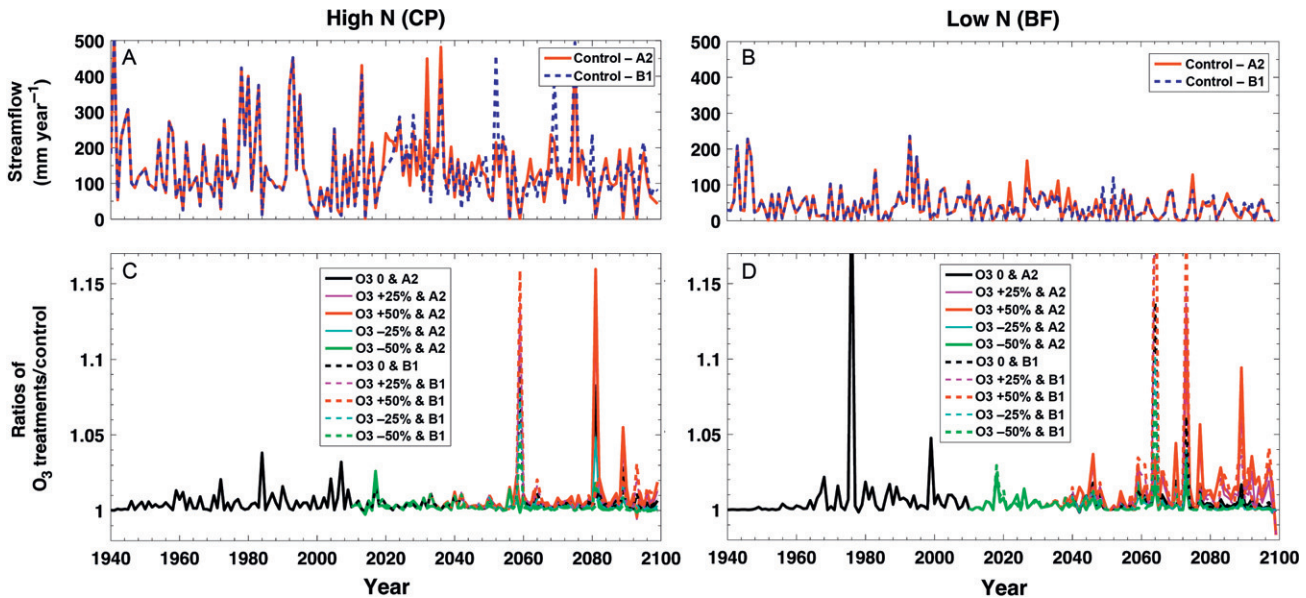


**FIGURE 16.7** DAYCENT simulated streamflow (soil drainage and runoff ) under CC, N deposition, and $O_3$ effects in SBM. See Figure 16.4 for details of the treatments.

(<5%) and occurred much later (abound 2000–2004) at the low N (cold and dry) BF site (Figure 16.4D). Simulations indicated that $O_3$ impacts on forest growth were closely related to N deposition in this N growth-limited ecosystem. If the current trend of decreases in $O_3$ continue, tree biomass would not change significantly even under climate warming at the high N site (CP), although at the low N site forest trees would recover from biomass loss in the late twenty-first century. Under the increasing $O_3$ scenarios (increases of 25% and 50%), tree biomass would decrease by another 9–10% and 4–5% by 2099 at CP and BF, respectively, for the A2 (medium–high emissions) climate-warming projection. The reduction in tree growth would be about 30–50% less for the B1 (low emissions) projection. If technology and/or policy management advances in the future decrease $O_3$ levels by 25% and 50%, $O_3$ effects would be minimized by the end of this century.

The DayCent simulations showed similar patterns of $O_3$ effects on soil organic matter (SOM) (Figure 16.5) as on tree biomass (Figure 16.4), but with smaller reductions (decreased by almost half as much as the effects on tree biomass) (Figure 16.5C and D). The simulations also showed small differences in $O_3$ effects on SOM at BF between the warmer A2 and colder B1 projection compared to the CP site. The simulations by Arbaugh et al. (1999) showed a larger increase of litterfall and litter biomass accumulation due to $O_3$ injury to foliage and thus almost no change in SOM. In our study, the $O_3$-caused reduction of tree biomass production resulted in decreased litterfall. This overall biomass reduction effect on litterfall was larger than the increase in litterfall resulting from $O_3$ injury to foliage. Therefore, the overall C input into SOM was less than for the non-$O_3$ simulations.

As expected, foliar injury and reduction in tree productivity by $O_3$ exposure caused decreases in plant transpiration of up to 4% during the historically high $O_3$ exposure period at CP, and up to 3% at BF (Figure 16.6C and D). Again the simulations showed less $O_3$ impact at the low N, cold and dry BF site. The decline in $O_3$ levels since the 1980s caused a recovery in transpiration capacity almost a decade later, which is maintained at 1–2% reduction at the high N CP site and less than 1% at the low N BF site, if the current trend of declining $O_3$ continues. The scenarios with projected $O_3$ increases result in larger reductions in plant transpiration under the two climate-warming projections. The difference between the two climate-warming projections on plant transpiration appeared small although the warmer A2 projections would have slightly larger transpiration loss.

The 1–2% (at most 5%) reduction in annual transpiration (15–40 mm at CP and 5–30 mm at BF, Figure 16.6A and B) caused by increased $O_3$ (Figure 16.6C and D) would not significantly impact the overall hydrological status of those sites in the future. For example, streamflow from soil drainage and runoff was about 143 mm at CP (wetter and warmer) and 72 mm at BF site (dryer and colder) (Figure 16.7A and B). Thus the 1–2% reduction of transpiration water loss by $O_3$ effects would have little effect on streamflow

in the normal and wet years. However, elevated $O_3$ would affect streamflow in drought years (Figure 16.7C and D). Under the future climate-warming conditions, streamflow could increase by as much as 15% during extremely dry years if the current $O_3$ levels increase by 50%.

At the high N and wet CP site, the simulation exhibited slightly higher yearly maximal stream $NO_3^-$ concentrations compared to the low N and dry BF site. However, at both sites, $NO_3^-$ concentrations increase with time, presumably as N was accumulating in the ecosystem as the current deposition rate was maintained. During events with streamflow lower than 1 mm, abnormally high $NO_3^-$ concentrations were projected because of high $NO_3^-$ content in lower soil layers. These artificially high values were not included in projections of yearly maximal streamflow $NO_3^-$ concentrations. Due to drier conditions at BF, the frequency of such events was much greater than at CP (Figure 16.8A and B).

As described earlier, $O_3$ effects on tree growth, SOM accumulation, and hydrology were larger at the high N site (CP, wetter and warmer) than the low N site (BF, drier and colder) but with similar response patterns to the $O_3$ changes and levels. In contrast, the response of nitrate ($NO_3^-$) concentrations in streamflow to $O_3$ showed an opposite effect at CP and BF (Figure 16.8C and D). Nitrate concentrations in the increasing $O_3$ scenarios were up to 9% higher than the non-$O_3$ simulation (control) during the historically high $O_3$ period at the high N and wet CP site (Figure 16.8C); while at the low N and dry BF site, such changes did not occur (Figure 16.8D). Secondly, at the high N and wet CP site, the projected higher $O_3$ levels are expected to result in higher $NO_3^-$ concentrations than the lower $O_3$ scenario (Figure 16.8C); while at the low N and dry BF site, $O_3$ levels showed an opposite effect on nitrate (Figure 16.8D). These responses essentially are the net result of two reverse $O_3$ effects of $O_3$ on $NO_3^-$ concentration. On the one hand, $O_3$ causes foliar injury, thus reducing plant transpiration, resulting in higher streamflow (hydrological aspect of $O_3$ effects); on the other hand, $O_3$ reduces plant production, consequently decreasing N uptake by trees and increasing N export into streamflow ('BGC aspect' of $O_3$ effects). Our results suggest that the BGC aspect of $O_3$ effects dominated N streamflow export under high N deposition during the historically high $O_3$ period and is projected to do so in the future. Conversely, the $O_3$-induced hydrological effect is expected to dominate the $O_3$ effect in determining streamflow nitrate under low N deposition conditions.

## 16.6 PROJECTING HYDROLOGICAL, NUTRITIONAL AND GROWTH RESPONSES OF FORESTED WATERSHEDS AT THE HUBBARD BROOK EXPERIMENTAL FOREST, REFLECTIVE OF THE AMERICAN NORTHEAST

Global change in the north-eastern United States is and will likely continue to be manifested in the future through increasing atmospheric concentrations of

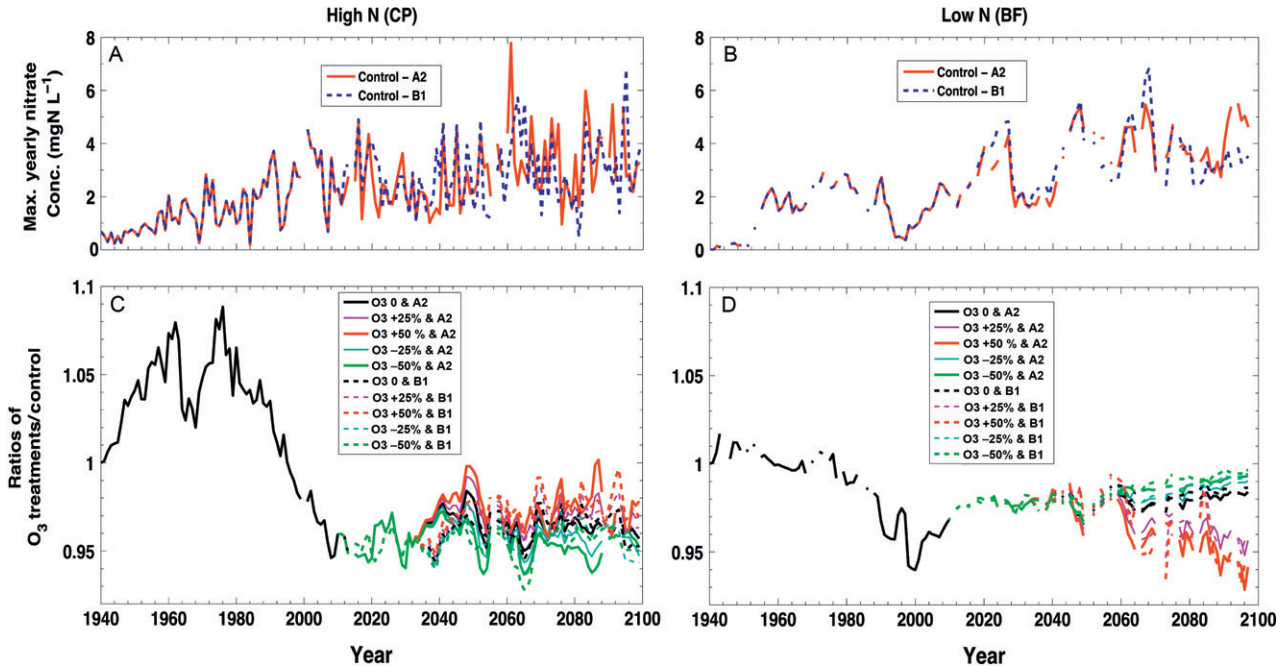


**FIGURE 16.8** DAYCENT simulated yearly maximal nitrate concentration in streamflow (events >1 mm) water under climate changes, N deposition and ozone effects in SBM. See Figure 16.4 for details of the treatments.

$CO_2$; increases in air temperature, less precipitation as snow and more as rain; decreases in snow cover; earlier arrival of spring and following snowmelt and earlier high spring river flows; a longer growing season; increases in storms and extreme events; and associated alterations in soil and surface water chemistry among other perturbations (Intergovernmental Panel on Climate Change (IPCC), 2007; NECIA, 2006).

In this study, we assess the potential effects of three contrasting N emission hindcast and future scenarios in conjunction with changes in climatic drivers (temperature, precipitation, and solar radiation) to the Northern Forest. We examine possible future CC scenarios, $CO_2$, and atmospheric nitrogen (N) deposition at the Hubbard Brook Experimental Forest (HBEF), New Hampshire, United States of America, as a case study, using the biogeochemical model PnET-BGC. A unique aspect of this case study is consideration of the simultaneous interactions of effects of $CO_2$ on vegetation (fertilization and response of stomatal conductance) and the potential for drought associated with higher temperature (and decreases in stomatal conductance) under contrasting conditions of N emissions and deposition (stimulating forest growth and carbon uptake, and perturbations to the acid–base chemistry of soil and surface waters). As with the previous case study, these drivers of global change (i.e. changes in temperature, precipitation, $CO_2$, and N deposition) can affect forest growth and associated C sequestration, hydrology and N cycling in unexpected ways. The application of PnET-BGC helps better understand the individual and combined effects of these drivers on forest ecosystem structure and function.

The HBEF is located in the southern White Mountains (43°56′N, 71°45′W) (Likens and Bormann, 1995). The site was established by the U.S. Forest Service in 1955 as a centre for hydrological research, and in 1987 was designated as a National Science Foundation Long-Term Ecological Research (LTER) site. The climate is humid continental, with short, cool summers and long, cold winters. The model was run for Watershed 6 (W6) which is a reference watershed. Watershed 6 has one of the longest continuous records of meteorology, hydrology and biogeochemistry in the United States (Likens and Bormann, 1995; Likens et al., 1994) (http://www.hubbardbrook.org/). The watershed area is 13.2 ha, with an elevation range of 549–792 m. Watershed 6 was logged intensively from 1910 to 1917, and has experienced subsequent disturbances including a hurricane in 1938, which prompted some salvage logging, and an ice-storm in 1998 without salvage logging. The dominant vegetation is northern hardwoods.

PnET-BGC is a BGC model that has been used to evaluate the effects of CC, atmospheric deposition and land disturbance on soil and surface waters in northern forest ecosystems (Chen and Driscoll, 2005). PnET-BGC was created by linking the forest–soil–water model PnET-CN (Aber and Driscoll, 1997; Aber et al., 1997), with a (BGC sub-model (Gbondo-Tugbawa et al., 2001), thereby enabling the simultaneous simulation of hydrology and major

element cycles ($Ca^{2+}$, $Mg^{2+}$, $K^{+}$, $Na^{+}$, C, N, P, S, Si, $Al^{3+}$, $Cl^{-}$, and $F^{-}$). PnET-BGC has been used to evaluate fluxes of water and elements in forest ecosystems by depicting ecosystem processes, including atmospheric deposition, $CO_2$, and tropospheric $O_3$ effects on vegetation, canopy interactions, plant uptake, litterfall, SOM dynamics, nitrification, mineral weathering (kept constant during the simulation), chemical reactions involving gas, solid and solution phases, and surface water processes (Gbondo-Tugbawa et al., 2001). These processes determine the hydrochemical characteristics of the ecosystem because water and solutes interact with forest vegetation and soil before emerging as surface runoff. A detailed description of PnET-BGC is provided by Aber and Driscoll (1997), Aber et al. (1997), and Gbondo-Tugbawa et al. (2001), including a sensitivity analysis of parameters.

In this application, the model was run on a monthly time step. Simulation from the year 1000 to 1850 is a spin-up period to allow the forest ecosystem to come to steady-state with respect to pre-anthropogenic climate and atmospheric deposition conditions. From 1850 to 2012, the model simulates hindcast conditions of changes in atmospheric deposition, meteorology, and land disturbance which are reconstructed from historical conditions (Gbondo-Tugbawa et al., 2001; Pourmokhtarian et al., 2012). The model was run as a forecast from 2012 through 2100 using future global change scenarios that are based on projected changes in climate, atmospheric $CO_2$, and three scenarios for atmospheric N emissions and deposition. The first N deposition scenario (N1) is 'business as usual' which includes our reconstruction of past atmospheric N deposition and no change in future atmospheric deposition of $NO_3^{-}$ and $NH_4^{+}$; the average of measured atmospheric deposition for 2001–2011 repeated from the year 2012 to 2100. The second scenario (N2) is 'background N deposition;' pre-anthropogenic atmospheric deposition of N is considered through the entire simulation period (1000–2100). The third scenario (N3) includes the hindcast of past atmospheric N deposition and a forecast of $NO_3^{-}$ deposition decreasing from the year 2012 to 2020 to background values and keeping this value constant through 2100 while $NH_4^{+}$ deposition remains 'business as usual'. The N3 scenario is established to depict aggressive controls on oxidized N emissions with no control on reduced N. Note that atmospheric deposition of all other elements were considered business as usual from the year 2012 to 2100. Details on input data, climate projections, spin-up period, and sensitivity of the model to climatic drivers are provided by Pourmokhtarian et al. (2012). The PnET-BGC is an open source model available to the public at http://www.lcs.syr.edu/faculty/driscoll/personal/PnET%20BGC.asp.

The depiction of the effects of increasing atmospheric $CO_2$ on trees is based on multi-layered sub-model of photosynthesis and phenology developed by Aber et al. (1995, 1996) and modified by Ollinger et al. (1997, 2002). A detailed description of $CO_2$ effects on vegetation, the processes and parameters related to photosynthesis in the model and the sensitivity analysis

are described by Ollinger et al. (1997, 2002, 2009). For this analysis, we considered contrasting $CO_2$ effects scenarios. For the CC without $CO_2$ effect scenarios, we do not invoke the $CO_2$ effects algorithm, so under this condition, trees do not respond to changes in $CO_2$. For the CC with $CO_2$ effects, we simulate the response of forest growth and stomatal conductance to changes in $CO_2$ described earlier.

We used data from two atmosphere-ocean global circulation models (AOGCMs): (1) the United Kingdom Meteorological Office Hadley Centre Coupled Model, version 3 (HadCM3) (Pope et al., 2000) and (2) the U.S. Department of Energy/National Center for Atmospheric Research Parallel Climate Model (PCM) (Washington et al., 2000). We coupled the HadCM3 model with A1fi (fossil fuel-intensive) emission scenario (Nakićenović et al., 2000), and the PCM model with B1 emission scenarios to represent possible higher and lower greenhouse gas emission futures, respectively. Consequently, two CC scenarios were developed for this application (HadCM3-A1fi and PCM-B1). Monthly, coarse resolution AOGCM temperature, precipitation, and solar radiation output were statistically downscaled using Station-based Daily Asynchronous Regression for weather station 1 at the HBEF for the period of 1960–2100 (O'Brien et al., 2001). Note that we used the same CC scenarios for both model simulations with and without $CO_2$ effects and the only difference between these sets of simulations is activation of $CO_2$ effects on the vegetation algorithm in the model.

### 16.6.1 CC (Without $CO_2$ Effects on Vegetation)

Model simulations suggest that seasonal hydrological patterns will shift substantially under projected CC scenarios (Figures 16.9 and 16.10). Under HadCM3-A1fi, in the future spring, snowmelt will occur earlier. Low flows associated with enhanced evapotranspiration during the summer months will begin earlier in the spring and continue later into the fall. Future streamflow in late fall and early winter will increase because of decreases in snowpack accumulation due to warmer air temperatures and concurrent declines in the ratio of snow to rain (Figure 16.9). Model projections under the more modest PCM-B1 scenario show that there is no change in timing and magnitude of spring snowmelt, but fall high flows will occur earlier with greater magnitude. Under PCM-B1, the duration of summer low flows will decrease due to an increase in summer discharge relative to 1970–2000 values (Figure 16.10). Future model projections indicate increases in annual water discharge under both scenarios for 2070–2100 compared to 1970–2000, with the percentage increase higher under PCM-B1 (Figures 16.9 and 16.10). Model simulations suggest hydrologic responses to scenarios of N deposition are subtle (data not shown). Annual water discharge will increase slightly (~1%) under background N deposition scenario N2 due to limited N fertilization effects on plant growth and C storage and associated decrease in transpiration losses compared to the higher N deposition scenarios (N1, N3).

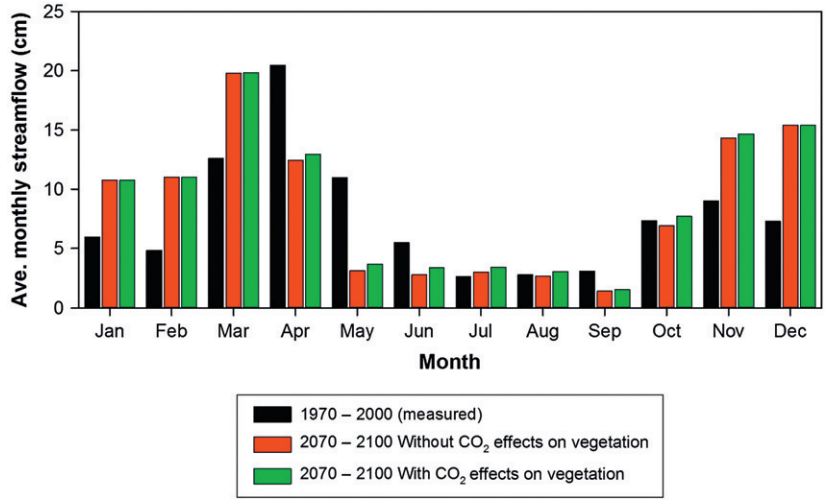


**FIGURE 16.9** Comparison between measured monthly discharge for 1970–2000 and simulated mean monthly discharge for 2070–2100 with and without considering $CO_2$ effects on vegetation. Note the future climate-change scenario depicted in these results is from HadCM3 A1fi with N emissions scenario of business as usual.

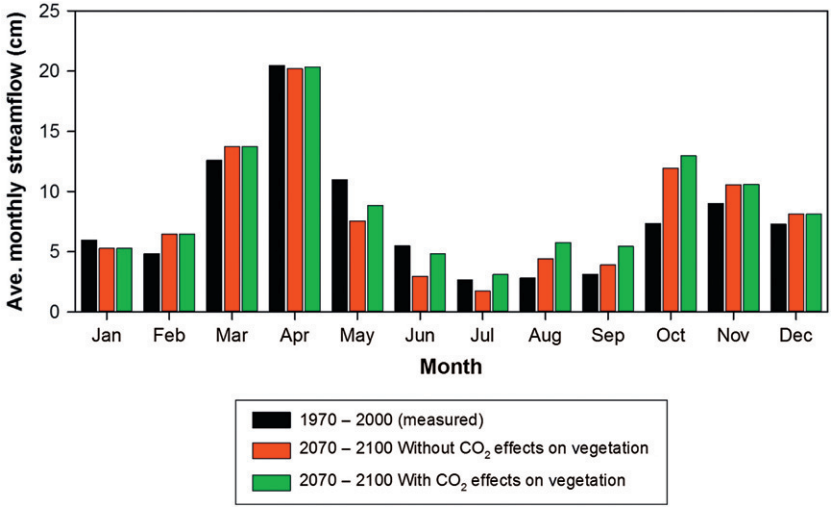


**FIGURE 16.10** Comparison between measured monthly discharge for 1970–2000 and simulated mean monthly discharge for 2070–2100 with and without considering $CO_2$ effects on vegetation. Note the future climate-change scenario depicted in these results is from PCM-B1 with N emissions scenario of business as usual.

The model simulations of forest vegetation without $CO_2$ effects showed future increases in NPP associated with warmer temperatures and lengthening of growing season for both climate scenarios. Under HadCM3-A1fi for N1, N2, and N3 deposition, the NPP increased by 14%, 10%, and 14%; 11%, 10%, and 11%; and 2%, 1%, and 1% over the 2010–2040, 2041–2070, and 2071–2100 periods, respectively, compared to 1970–2000 values. In comparison, the PCM-B1 scenario (with N1, N2, and N3 deposition) resulted in increases in the NPP (by 14%, 10%, and 14%), (9%, 5%, and 9%), and (13%, 9%, and 12%) over the same periods relative to 1970–2000 values (Figure 16.11A). This difference in response for the two CC scenarios is due to the forest ecosystem exceeding the optimum temperature for photosynthesis under HadCM3-A1fi which causes temperature stress to vegetation and mid-summer drought. Model simulations suggest that CC without $CO_2$ fertilization has a relatively small effect on NPP. Note, under both CC scenarios, NPP was lower under the N2 deposition scenario compared to N1 and N3. These results suggest that anthropogenic N deposition stimulates forest growth and C sequestration under CC.

Future model projections under both scenarios and all conditions (with and without $CO_2$ effects on vegetation) suggest that the soil N pool will decrease under changing climate, with the magnitude of N loss depending on the scenario (Figure 16.11B). Under HadCM3-A1fi, higher projected temperatures and associated increases in N mineralization and nitrification rates resulted in a decrease in the soil N pool of 51% by 2070–2100 compared to 1970–2000. Under the less severe PCM-B1 scenario, the average decline in soil N is considerably less (12%). The simulations suggest that CC will have the potential to shift the soil N humus pool from a net N sink to a N source. It is counterintuitive that there is no significant difference in the soil N pools among the three N deposition scenarios. The soil N pool is large ($\sim$330 g $m^{-2}$ $year^{-1}$) compared with the cumulative inputs of atmospheric N deposition from 1850 to 2100 under these scenarios (N1 = 106.5 g $m^{-2}$, N2 = 17.5 g $m^{-2}$ and N3 = 81 g $m^{-2}$).

Annual volume-weighted $NO_3^-$ concentrations are projected to increase under future CC with the magnitude of this response depending on the CC and N deposition scenario considered (Figure 16.11C). Under the HadCM3-A1fi and N1, annual volume-weighted $NO_3^-$ concentration peaked around 2047 and then declined towards 2100 (with the exception of one last sharp increase at 2096) associated with the long-term decreases in the soil humus N pool. In comparison, annual volume-weighted $NO_3^-$ concentration under PCM-B1 and N1 increased towards 2020, declined around 2025, and then increased (slope = 0.23 μmol $NO_3^-$ $L^{-1}$ $year^{-1}$) until 2100 (Figure 16.11C). The simulated increase in annual volume-weighted $NO_3^-$ concentrations is due to decreases in soil moisture and an increase in vapour pressure deficit, which occur despite the increase in precipitation, causing decreases in evapotranspiration and mid-summer drought. Drought stress disrupts tree N uptake

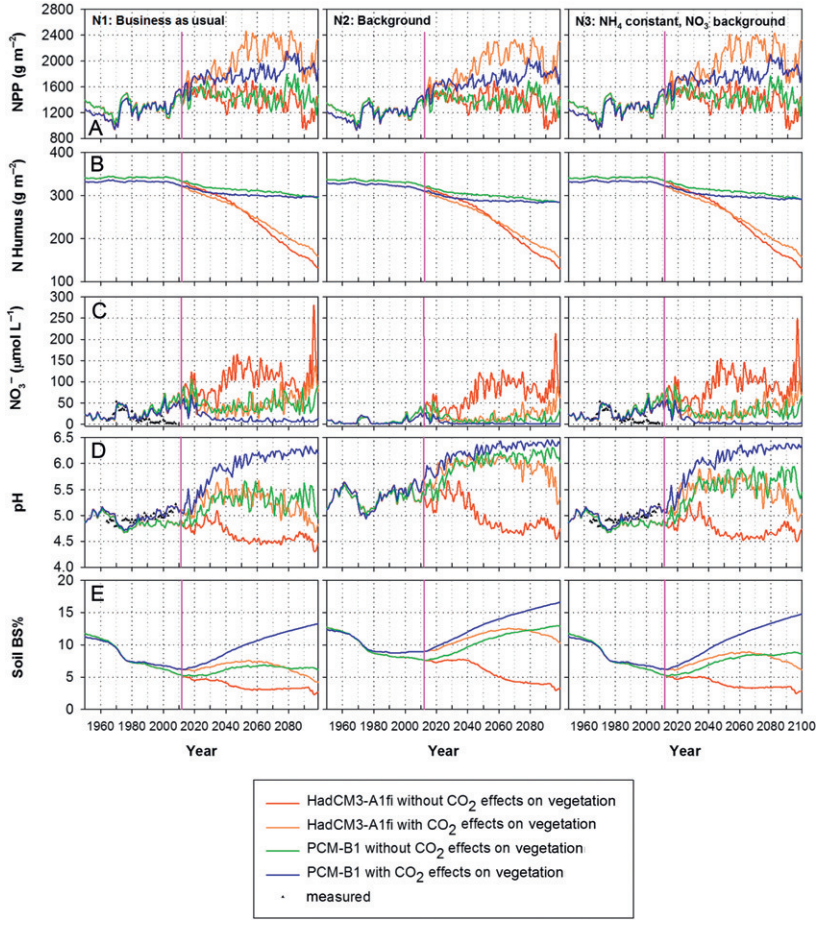


**FIGURE 16.11** Future projected changes in (A) net primary productivity (NPP), (B) N humus pool, (C) annual volume-weighted concentrations of $NO_3^-$, (D) pH, and (E) soil base saturation (BS%), under HadCM3-A1fi and PCM-B1 scenarios with and without considering $CO_2$ effects on vegetation. Measured data are shown.

from soil resulting in an increase in net N mineralization, nitrification, and elevated $NO_3^-$ leaching (Pourmokhtarian et al., 2012). The scenario of background N deposition (N2) also shows large increases in the magnitude of annual volume-weighted $NO_3^-$ concentration (e.g. under HadCM3-A1fi; 6.4 µmol $L^{-1}$ for 1970–2000 to 89 µmol $L^{-1}$ for 2070–2100; more than one order of magnitude) (Figure 16.11C). Nevertheless, these elevated $NO_3^-$ concentrations are still lower than values under comparable CC but higher N deposition scenarios (N1 and N3). These results suggest that historical increases in atmospheric N deposition to the Northern Forest are manifested

through an increase in stream water $NO_3^-$ concentration. Moreover, these legacy effects of atmospheric N deposition may be realized in the future under CC with elevated $NO_3^-$ leaching associated with increases in net soil mineralization and nitrification.

Future model projections of pH exhibit patterns that followed changes in stream $NO_3^-$ (Figure 16.11D). The average annual volume-weighted pH projected for 2070–2100 under HadCM3-A1fi and N1 decrease by up to 0.3 pH unit coinciding with high stream $NO_3^-$ compared to average of measured values (4.9) for 1970–2000. Under PCM-B1 and N1 for the same period, pH increases by up to 0.5 pH unit.

Soils at the HBEF are inherently acidic (low % BS) and sensitive to the effects of acidic deposition. Simulations of soil base saturation (BS %) are projected to decrease by almost 58% and 12% under the HadCM3-A1fi and PCM-B1 scenarios with N1, respectively (Figure 16.3E). The model projections for HadCM3-A1fi showed a 55% decrease in soil BS% under both N2 and N3, while under PCM-B1 scenario, the soil BS% increased by 43% and 17%, respectively (Figure 16.11E). These results suggest that under moderate temperature CC scenarios, the future controls on N emissions could play an important role in the recovery of the acid–base status of forest ecosystems. In contrast, under high-temperature scenarios, the high rate of soil N mineralization, nitrification, and associated acidification due to the accumulation of legacy N from past elevated deposition could overwhelm any benefits of potential future controls on $NO_x$ emissions.

### 16.6.2 CC with $CO_2$ Effects

Model results with $CO_2$ effects on vegetation showed that increasing $CO_2$ uptake by vegetation had little impact on the seasonal patterns of streamflow, causing only a slight increase in the annual discharge (Figures 16.9 and 16.10).

Invoking $CO_2$ fertilization effects on the forest ecosystem causes substantial increases in the NPP (68% and 49% for HadCM3-A1fi (N1) and PCM-B1 (N1), respectively for 2070–2100 compared to 1970–2000; Figure 16.11A). Elevated $CO_2$ decreases stomatal conductance and increases tree growth which increases water use efficiency (WUE) and annual water yield, limiting the occurrence of mid-summer drought. This effect is more evident under PCM-B1. Under the more severe HadCM3-A1fi scenario (N1), $CO_2$ effects on tree growth are projected to plateau towards the end of century (2080–2090) due the non-linear response of photosynthesis to $CO_2$ (at concentrations above 600 ppm). After $CO_2$ effects on forest vegetation play out, temperature increases become the dominant driver, promoting recurring drought (Pourmokhtarian et al., 2012). This response is important considering the importance of northern hardwood forests to the north-eastern United States and services they provide. The responses of NPP are largely driven by climate and $CO_2$ effects and the effects of N deposition are minimal.

Modelling results suggest that invoking $CO_2$ effects on vegetation has little impact on soil N humus due to the large size of the pool (Figure 16.11B). Under the HadCM3-A1fi scenario, the rate of decline in the N humus pool is lower by around 10% (42% compared to 51%) due to enhanced $CO_2$ uptake by trees.

The projected future increases in annual volume-weighted $NO_3^-$ concentrations diminished substantially due to enhanced growth of trees and higher nutrient uptake associated with forest fertilization from $CO_2$ and the elimination of mid-summer drought caused by higher WUE due to decreases in stomatal conductance (Pourmokhtarian et al., 2012). Under the aggressive HadCM3-A1fi (N1) scenario, despite the enhanced tree growth associated with a $CO_2$ fertilization effect, the increase in temperature eventually increases net N mineralization and nitrification causing a condition of N saturation and resulting in annual volume-weighted $NO_3^-$ concentrations started to increase after 2035 (Figure 16.11C). Stream water pH projections for 2070–2100 showed increases by up to 0.6 and 0.9 pH unit compared to simulations without $CO_2$ effects under HadCM3-A1fi (N1) and PCM-B1 (N1) scenarios, respectively (Figure 16.11D). The soil BS% under $CO_2$ effects is projected to increase substantially, with the magnitude and extent of the increases depending on the CC and N deposition scenario considered (Figure 16.11E). The greatest increases in soil %BS under the $CO_2$ fertilization effect occurred under PCM-B1 and N2, while the smallest increases occurred under HadCM3-A1fi and N1.

## 16.7 CONCLUSIONS

This chapter illustrates close linkages between CC and air pollution effects in forest ecosystems. These linkages are manifested in complex patterns which alter the structure and function of forests and potentially associated ecosystem services. Although the case studies presented represent contrasting forest ecosystems and disturbance regimes, there are some common features to the hindcasts and projections provided. CC (changes in temperature and precipitation), increasing $CO_2$ levels, changes in $O_3$ concentrations, and N deposition all can affect tree growth and therefore influence important ecosystem services such as C sequestration, water quantity, and soil and water quality.

In southern California, mixed conifer forest concentrations of $O_3$ have been historically high, resulting in severe damage of sensitive trees and extended dieback of forest stands. These high $O_3$ values have recently decreased, and it is anticipated that these trends will continue in the coming decades. It is expected that $O_3$ will interact with CC to strongly influence important ecosystem function such as C sequestration, and the quantity, distribution, and quality of stream water. Forest nutritional status, especially in terms of N nutrition, can have major effects on forest responses to $O_3$. Simulation of future changes in mixed conifer forests of southern California implies that $O_3$ impacts on forest growth are closely associated with

N deposition in these N-limited ecosystems. If the current trend of decreases in $O_3$ continues, tree biomass would not change significantly even under climate warming at high N deposition although at low N deposition forest trees would recover from biomass loss in the late twenty-first century. Under the increasing $O_3$ scenarios used, tree biomass would decrease at both N deposition projections, but much more for the A2 (medium–high emissions) climate-warming projection than at the B1 (low emissions) projection. If technology and/or policy management advances in the future decrease $O_3$ levels, its negative effects could be minimized by the end of this century. However, these positive changes can be negated by higher efficiency of $O_3$ photochemical production due to increasing temperatures.

The northern forests have been historically impacted by acidic deposition, which has acidified soil and surface waters, impacted the health of sensitive tree species, and altered the diversity of aquatic biota. In recent decades, emission controls on $SO_2$ and $NO_x$ have diminished the impacts of acidification. CC has and will alter hydrology, decrease C and N sequestration, and potentially mobilize soil N resulting in the re-acidification of soil and water. The extent of these effects will likely vary depending on the future CC and N emission and deposition scenario as well as the extent to which increases in $CO_2$ stimulate additional tree growth. Negative impacts of acidic deposition could also be reduced by increased mineral weathering and availability of base cations caused by future higher temperatures.

## 16.8 RESEARCH AND MANAGEMENT NEEDS

Long-term monitoring of ground-level background $O_3$ and development of physiologically relevant $O_3$ indices are needed to verify model outputs and understand future $O_3$ risks to forests. Improved remote sensing techniques are needed to estimate air pollutant exposure in remote areas. Such techniques would greatly expand our ability to evaluate risks caused by toxic gases and atmospheric deposition in forests and other ecosystems. Future research is needed to better establish the role of fires and vertical transport of $O_3$ from the free troposphere to the boundary layer on ground-level $O_3$ exposure regimes. These issues are important factors for increasing our understanding of $O_3$ threats to U.S. ecosystems, especially in complex, mountainous terrain.

Improved assessments of increasing springtime $O_3$ concentrations on plant performance are needed. $O_3$ response models in North America should be modified to include the entire physiologically active period that is changing with a warming climate. While we recommend the continuing use of $O_3$ exposure indices developed in the United States, we also support testing and development of other approaches, such as those already developed in Europe (effective $O_3$ flux approaches). These should be tested and possibly developed for key tree species in various U.S. ecological zones. Improved understanding of gas exchange and biochemical defence mechanisms of key tree species is

needed for understanding effective $O_3$ flux and its risks to forests. In this context, the effects of $O_3$ on the gas exchange capacity of trees, especially the question of potential stomatal sluggishness caused by chronic $O_3$ exposures, are a key issue for projecting the capacity of forests to sequester $CO_2$, for projecting potential growth, and effects on water fluxes in forest stands and catchments.

Better understanding of spatial and temporal distribution of N dry deposition and of key drivers of deposition, such as $NH_3$, $HNO_3$, and $NO_2$, as well as $NO_3^-$ and $NH_4^+$ particulate matter, are needed for identification of sources of pollution and to develop options for their control. Similarly, better characterization of cloud water deposition of inorganic and organic reactive N species is needed. There is also a need for better models to describe deposition of reactive N species to forests in remote areas (especially complex mountain terrain). This will require better inventories of N emissions (especially reduced forms of N) and improved understanding of meteorological, chemical, and transport processes and their integration. Such models should be compared with empirical deposition data and new GIS-based inferential N deposition models as well as results of dry deposition measurements obtained with relax eddy flux methodologies.

Models are critical tools to assess CC effects on ecosystem structure and function. Robust holistic models are required to evaluate interactive effects of multiple air pollutants, ecosystem nutrient status (including the $CO_2$ fertilization effect), CC, management practices, and various other biotic and abiotic stressors. Models that simulate the responses of individual tree species and community responses to these factors are needed. Regional and global models of hydrologic cycles and related ecosystem functions should consider potential interactions of $O_3$ with future CC. In particular, it is important that experimental forest watersheds such as those used in the case studies in this chapter be maintained and preserved. Intensive monitoring and long-term measurements of meteorology, air quality, forest biomass, hydrology, and water quality at experimental watersheds are essential for the parameterization and testing of models used to predict the effects of CC and air pollution. This work should be supported and expanded in the future.

## ACKNOWLEDGEMENTS

Work by A. P. and C. T. D. was supported by the USEPA through the STAR Program and by the NSF through the LTER program.

## REFERENCES

Aber, J.D., Driscoll, C.T., 1997. Effects of land use, climate variation, and N deposition on N cycling and C storage in northern hardwood forests. Glob. Biogeochem. Cycles 11 (4), 639–648. http://dx.doi.org/10.1029/97GB01366.

Aber, J.D., Ollinger, S.V., Federer, C.A., Reich, P.B., Goulden, M.L., Kicklighter, D.W., Melillo, J.M., Lathrop Jr., R.G., 1995. Predicting the effects of climate change on water yield

and forest production in the northeastern United States. Climate Res. 05 (3), 207–222. http://dx.doi.org/10.3354/cr0005207.

Aber, J.D., Reich, P.B., Goulden, M.L., 1996. Extrapolating leaf $CO_2$ exchange to the canopy: a generalized model of forest photosynthesis compared with measurements by Eddy correlation. Oecologia 106 (2), 257–265. http://dx.doi.org/10.1007/BF00328606.

Aber, J.D., Ollinger, S.V., Driscoll, C.T., 1997. Modeling nitrogen saturation in forest ecosystems in response to land use and atmospheric deposition. Ecol. Model. 101 (1), 61–78. http://dx.doi.org/10.1016/S0304-3800(97)01953-4.

Aber, J.D., Neilson, R., McNulty, S.G., Lenihan, J., Bachelet, D., Drapek, R., 2001. Forest processes and global environmental change: predicting the effects of individual and multiple stressors. Bioscience 59, 735–751.

Ainsworth, E.E., Yendrek, C.R., Sitch, S., Collins, W.J., Emberson, L.D., 2012. The effects of tropospheric ozone on net primary productivity and implications for climate change. Annu. Rev. Plant Biol. 63, 637–661.

Arbaugh, M.J., Miller, P.R., Carroll, J.J., Takemoto, B., Procter, T.M., 1998. Relationships of ozone exposure to pine injury in the Sierra Nevada and San Bernardino Mountains of California. Environ. Pollut. 101, 291–301.

Arbaugh, M.J., Johnson, D.W., Pulliam, W.M., 1999. Simulated effects of N deposition, ozone injury and climate change on a forest stand in the San Bernardino Mountains. In: Oxidant Air Pollution Impacts in the Montane Forests of Southern California: A Case Study of the San Bernardino Mountains. Springer-Verlag, New York, pp. 353–372.

Brasseur, G.P., Muller, J.-F., Tie, X., Horowitz, L., 2001. Tropospheric ozone and climate: past, present and future. In: Matsuno, T., Kida, H. (Eds.), Present and Future of Modeling Global Environmental Change: Toward Integrated Modeling. TERRAPUB, Tokyo, pp. 63–75.

Brimblecombe, P., 1987. The Big Smoke. Taylor & Francis Group, London, p. 185.

Bytnerowicz, A., Dueck, T., Godzik, S., 1998. Nitric oxide, nitrogen dioxide, nitric acid vapor and ammonia. In: Flagler, R. (Ed.), Recognition of Air Pollution Injury to Vegetation: A Pictorial Atlas. Air & Waste Management Association, Pittsburgh, PA, 5-1 through 5-17.

Bytnerowicz, A., Omasa, K., Paoletti, E., 2007. Integrated effects of air pollution and climate change on forests: a Northern Hemisphere perspective. Environ. Pollut. 147, 438–445.

Bytnerowicz, A., Arbaugh, M., Schilling, S., Fraczek, W., Alexander, D., 2008. Ozone distribution and phytotoxic potential in mixed conifer forests of the San Bernardino Mountains, southern California. Environ. Pollut. 155, 398–408.

CASTNET, 2012. Clean Air Status and Trends Network (CASTNET) 2010 Annual Report. Prepared by AMEC Environment & Infrastructure, Inc., for U.S. Environmental Protection Agency, EPA Contract No. EP-W-09-028, Washington, DC, April 2012.

Cayan, D.R., Maurer, E.P., Dettinger, M.D., Tyree, M., Hayhoe, K., 2008. Climate change scenarios for the California region. Clim. Change 87 (Suppl. 1), S21–S42.

Chen, L., Driscoll, C.T., 2005. A two-layer model to simulate variations in surface water chemistry draining a northern forest watershed. Water Resour. Res. (W09425) 41 (9), 8. http://dx.doi.org/10.1029/2004WR003625.

Cooper, O.R., Parrish, D.D., Stohl, A., Trainer, M., Nédélec, P., Thouret, V., Cammas, J.P., Oltmans, S.J., Johnson, B.J., Tarasick, D., Leblanc, T., McDermid, I.S., Jaffe, D., Gao, R., Stith, J., Ryerson, T., Aikin, K., Campos, T., Weinheimer, A., Avery, M.A., 2010. Increasing springtime ozone mixing ratios in the free troposphere over western North America. Nature 463, 344–348.

Davidson, E.A., David, M.B., Galloway, J.N., Goodale, C.L., Haueber, R., Harrson, J.A., Howarth, R.W., Jaynes, D.B., Lowrance, R.R., Nolan, B.T., Peel, J.L., Pinder, R.W.,

Porter, E., Snyder, C.S., Townsend, A.R., Ward, M.H., 2012. Excess nitrogen in the U.S. environment: trends, risks, and solutions. Issues Ecol. 15, 16.

Del Grosso, S.J., et al., 2000. General model for $N_2O$ and $N_2$ gas emissions from soils due to denitrification. Global Biogeochem. Cycle 14, 1045–1060.

Doherty, R.M., Wild, O., Shindell, D.T., Zeng, G., MacKenzie, I.A., Collins, W.J., Fiore, A.M., Stevenson, D.S., Dentener, F.J., Schultz, M.G., Hess, P., Derwent, R.G., Keating, T.J., 2013. Impacts of climate change on surface ozone and intercontinental ozone pollution: a multi-model study. J. Geophys. Res. Atmos. 118, 3744–3763.

Fasullo, J.T., Trenberth, K.E., 2012. A less cloudy future: the role of subtropical subsidence in climate sensitivity. Science 338, 792–794.

Felzer, B., Kicklighter, D., Melillo, J., Wang, C., Zhuang, Q., Prinn, R., 2004. Effects of ozone on net primary production and carbon sequestration in the conterminous United States using a biogeochemistry model. Tellus 56B, 230–248.

Fenn, M.E., Baron, J.S., Allen, E.B., Rueth, H.M., Nydick, K.R., Geiser, L., Bowman, W.D., Sickman, J.O., Meixner, T., Johnson, D.W., Neitlich, P., 2003. Ecological effects of nitrogen deposition in the western United States. Bioscience 53, 404–420.

Fenn, M.E., Jovan, S., Yuan, F., Geiser, L., Meixner, T., Gimeno, B.S., 2008. Empirical and simulated critical loads for nitrogen deposition in California mixed conifer forests. Environ. Pollut. 155, 492–511.

Fourier, J., 1824. Remarques Générales Sur Les Températures Du Globe Terrestre Et Des Espaces Planétaires. Annal. Chim. Phys. 27, 136–167.

Gauss, M., et al., 2003. Radiative forcing in the 21st century due to ozone changes in the troposphere and the lower stratosphere. J. Geophys. Res. 108 (D9), 4292.

Gauss, M., Myhre, G., Isaksen, I.S.A., Grewe, V., Pitari, G., Wild, O., Collins, W.J., Dentener, F.J., Ellingsen, K., Gohar, L.K., Hauglustaine, D.A., Iachetti, D., Lamarque, J.-F., Mancini, E., Mickley, L.J., Prather, M.J., Pyle, J.A., Sanderson, M.G., Shine, K.P., Stevenson, D.S., Sudo, K., Szopa, S., Zeng, G., 2006. Radiative forcing since preindustrial times due to ozone change in the troposphere and the lower stratosphere. Atmos. Chem. Phys. 6, 575–599.

Gbondo-Tugbawa, S.S., Driscoll, C.T., Aber, J.D., Likens, G.E., 2001. Evaluation of an integrated biogeochemical model (PnET-BGC) at a northern hardwood forest ecosystem. Water Resour. Res. 37 (4), 1057–1070. http://dx.doi.org/10.1029/2000WR900375.

Greaver, T.L., Sullivan, T.J., Herrick, J.D., Barber, M.C., Baron, J.S., Cosby, B.J., Deerhake, M.E., et al., 2012. Ecological effects of nitrogen and sulfur air pollution in the US: what do we know? Front. Ecol. 10 (7), 365–372.

Grulke, N.E., Balduman, L., 1999. Deciduous conifers: high N deposition and $O_3$ exposure effects on growth and biomass allocation in ponderosa pine. Water Air Soil Pollut. 116, 235–248.

Grulke, N.E., Paoletti, E., Heath, R.L., 2006. Direct measurements of foliar ozone uptake in crop and tree species. Environ. Pollut. 146, 640–647.

Grulke, N.E., Minnich, R.A., Paine, T.D., Seybold, S.J., Chavez, D.J., Fenn, M.E., Riggan, P.J., Dunn, A., 2009. Air pollution increases forest susceptibility to wildfires: a case study in the San Bernardino Mountains in southern California. In: Bytnerowicz, A., Arbaugh, M.J., Riebau, A.R., Andersen, C. (Eds.), Wildland Fires and Air Pollution. Developments in Environmental Science, vol. 8. Elsevier, Amsterdam, pp. 365–403.

Intergovernmental Panel on Climate Change (IPCC), 2000. IPCC Special Report Emission Scenarios. Summary for Policymakers. UNEP, WMO, Geneva, p. 20.

Intergovernmental Panel on Climate Change (IPCC), 2007. In: Solomon, S., Qin, D., Manning, M., Chen, Z., Marquis, M., Averyt, K.B., Tignor, M., Miller, H.L. (Eds.), Climate Change 2007:

The Physical Science Basis. Contribution of Working Group I to the Fourth Assessment Report of the Intergovernmental Panel on Climate Change. Cambridge University Press, Cambridge, United Kingdom and New York, NY, USA.

Jacob, D.J., Winner, D.A., 2009. Effect of climate change on air quality. Atmos. Environ. 43 (1), 51–63. http://dx.doi.org/10.1016/j.atmosenv.2008.09.051.

Karl, T.R., Melillo, J.M., Peterson, T.C. (Eds.), 2009. Global Climate Change Impacts in the United States. Cambridge University Press, London England, p. 188.

Kurpius, M.R., Goldstein, A.H., 2003. Gas-phase chemistry dominates $O_3$ loss to a forest, implying a source of aerosols and hydroxyl radicals to the atmosphere. Geophys. Res. Lett. 30 (7), 1371. http://dx.doi.org/10.1029/2002GL016785.

Law, K., 2010. More ozone over North America. Nature 463, 307–308.

Lefohn, A.S., Laurence, J.A., Kohut, R.J., 1988. A comparison of indices that describe the relationship between exposure to ozone and reduction in the yield of agricultural crops. Atmos. Environ. 22, 1229–1240.

Lefohn, A.S., Shadwick, D., Oltmans, S.J., 2008. Characterizing long-term changes in surface ozone levels in the United States (1980–2005). Atmos. Environ. 42, 8252–8262.

Legge, A.H., Jäger, H.-J., Krupa, S.V., 1998. Sulfur dioxide. In: Flagler, R.B. (Ed.), Recognition of Air Pollution Injury to Vegetation—A Pictorial Atlas. Air & Waste Management Association, Pittsburgh, PA, 3-1 through 3-42.

Lei, H., Wuebbles, D.J., Liang, X.-Z., 2012. Projected risk of high ozone episodes in 2050. Atmos. Environ. 59, 567–577.

Li, H., McNulty, S.G., 2007. Uncertainty analysis on simple mass balance model to calculate critical loads for soil acidity. Environ. Pollut. 149, 315–326.

Likens, G.E., Bormann, F.H., 1995. Biogeochemistry of a Forested Ecosystem, second ed. Springer-Verlag, New York, USA.

Likens, G.E., Driscoll, C.T., Buso, D.C., Siccama, T.G., Johnson, C.E., Lovett, G.M., Ryan, D.F., Fahey, T., Reiners, W.A., 1994. The biogeochemistry of potassium at Hubbard Brook. Biogeochemistry 25 (2), 61–125. http://dx.doi.org/10.1007/BF00000881.

Matyssek, R., Wieser, G., Calfapietra, C., de Vries, W., Dizengremel, P., Ernst, D., Jolivet, Y., Mikkelsen, T.N., Hohren, G.M.J., Le Thiec, D., Tuovinen, J.-P., Weatherall, A., Paoletti, E., 2012. Forests under climate change and air pollution: gaps in understanding and future directions for research. Environ. Pollut. 160, 57–65.

McDonald-Buller, E.C., Allen, D.T., Brown, N., Jacob, D.J., Jaffe, D., Kolb, C.E., Lefohn, A.S., Oltmans, S., Parrish, D.D., Yarwood, G., Zhang, L., 2011. Establishing policy relevant background (PRB) ozone concentrations in the United States. Environ. Sci. Technol. 45, 9484–9497.

McKenzie, D., Peterson, D.L., Littell, J.J., 2009. Global warming and stress complexes in forests of western North America. In: Bytnerowicz, A., Arbaugh, M.J., Riebau, A.R., Andersen, C. (Eds.), Wildland Fires and Air Pollution. Developments in Environmental Science, 8. Elsevier, Amsterdam, pp. 319–337.

McNulty, S.G., Boggs, J.L., 2010. A conceptual framework: redefining forest soils critical acid loads under a changing climate. Environ. Pollut. 158, 2053–2058.

McNulty, S.G., Cohen, E.C., Moore Myers, J.A., Sullivan, T.J., Li, H., 2007. Estimates of critical acid loads and exceedances for forest soils across the conterminous United States. Environ. Pollut. 149, 281–292.

Miller, P.R., Parmeter Jr., J.R., Taylor, O.C., Cardiff, E.A., 1963. Ozone injury to the foliage of *Pinus ponderosa*. Phytopathology 53, 1072–1076.

NADP, 2010. National Atmospheric Deposition Program. 2010 Annual Summary. Illinois State Water Survey, Urbana-Champaign, 23 pp.

Nakićenović, N., Alcamo, J., Davis, G., Vries, B.D., Fenhann, J., Gaffin, S., Gregory, K., Grübler, A., Jung, T.Y., Kram, T., 2000. In: Special Report on Emissions Scenarios: A Special Report of Working Group III of the Intergovernmental Panel on Climate Change, first ed. Cambridge University Press, Cambridge, UK/New York, NY.

Northeast Climate Impact Assessment (NECIA), 2006. Climate Change in the U.S. Northeast. A Report of the Northeast Climate Impacts Assessment. Union of Concerned Scientists (UCS), UCS Publications,, Cambridge, Massachusetts, USA.

O'Brien, T.P., Sornette, D., McPherron, R.L., 2001. Statistical asynchronous regression: determining the relationship between two quantities that are not measured simultaneously. J. Geophys. Res. 106 (A7), 13247–13259. http://dx.doi.org/10.1029/2000JA900193.

Ollinger, S.V., Aber, J.D., Reich, P.B., 1997. Simulating ozone effects on forest productivity: interactions among leaf-, canopy-, and stand-level processes. Ecol. Appl. 7 (4), 1237–1251.

Ollinger, S.V., Aber, J.D., Reich, P.B., Freuder, R.J., 2002. Interactive effects of nitrogen deposition, tropospheric ozone, elevated $CO_2$ and land use history on the carbon dynamics of Northern Hardwood Forests. Global Chang. Biol. 8 (6), 545–562.

Ollinger, S.V., Goodale, C.L., Hayhoe, K., Jenkins, J.P., 2009. Potential effects of climate change and rising $CO_2$ on ecosystem processes in northeastern U.S. forests. Mitig. Adapt. Strategies Global Change 14 (1), 101–106.

Oltmans, S.J., Lefohn, A.S., Shadwick, D., Harris, J.M., Scheel, H.E., Galbally, I., Tarasick, D.W., Johnson, B.J., Brunke, E.-G., Claude, H., Zeng, G., Nichol, S., Schmidlin, F., Davies, J., Cuevas, E., Redondas, A., Naoe, H., Nakano, T., Kawasato, T., 2013. Recent tropospheric ozone changes—a patterns dominated by slow or no growth. Atmos. Environ. 67, 331–351.

Pardo, L.H., Fenn, M.E., Goodale, C.L., Geiser, L.H., Driscoll, C.T., Allen, E.B., Baron, J., Bobbink, R., Bowman, W.D., Clark, C., Emmett, B., Gilliam, F.S., Greaver, T., Hall, S.J., Lilleskov, E.A., Liu, L., Lynch, J., Nadelhoffer, K., Perakis, S.S., Robin-Abbott, M.J., Stoddard, J., Weathers, K., Dennis, R.L., 2011. Effects of nitrogen deposition and empirical nitrogen critical loads for ecoregions of the United States. Ecol. Appl. 21 (8), 3049–3082.

Parton, W.J., Scurlock, J.M.O., Ojima, D.S., Gilmanov, T.G., Scholes, R.J., Schimel, D.S., Kirchner, T., Menaut, J.-C., Seastedt, T., Garcia-Moya Apinan-Kamnalrut, E., Kinyamario, J.I., 1993. Observations and modeling of biomass, soil organic matter dynamics for the grassland biome worldwide. Global Biogeochem. Cycles 7, 785–809.

Parton, W.J., Hartman, M., Ojima, D., Schimel, D.S., 1998. DAYCENT and its land surface submodel: description and testing. Glob. Planet Change 19, 35–48.

Parton, W.J., Holland, E.A., Del Grosso, S.J., Hartman, M.D., Martin, R.E., Mosier, A.R., Ojima, D.S., Schimel, D.S., 2001. Generalized model for $NO_x$ and $N_2O$ emissions from soils. J. Geophys. Res. (Atmospheres) 106, 17403–17419.

Peterson, D.L., Arbaugh, M., Robinson, L., 1991. Regional growth changes in ozone-stressed ponderosa pine (*Pinus ponderosa*) in the Sierra Nevada, California, USA. Holocene 1, 50–61.

Pinder, R.W., Bettez, N.D., Bonan, G.B., Greaver, T.L., Wieder, W.R., Schlezinger, W.H., Davidson, E.A., 2013. Impacts of human alterations of the nitrogen cycle in the US on radiative forcing. Biogeochemistry 114 (1–3), 25–40. http://dx.doi.org/10.1007/s10533-012-9787-z.

Pope, V.D., Gallani, M.L., Rowntree, P.R., Stratton, R.A., 2000. The impact of new physical parametrizations in the Hadley Centre Climate Model: HadAM3. Climate Dyn. 16 (2), 123–146. http://dx.doi.org/10.1007/s003820050009.

Post, W.M., Venterea, R.T., 2012. Managing biogeochemical cycles to reduce greenhouse gases. Front. Ecol. Environ. 10, 511.

Pourmokhtarian, A., Driscoll, C.T., Campbell, J.L., Hayhoe, K., 2012. Modeling potential hydrochemical responses to climate change and increasing $CO_2$ at the Hubbard Brook Experimental Forest using a dynamic biogeochemical model (PnET-BGC). Water Resour. Res. 48 (7). http://dx.doi.org/10.1029/2011WR011228, W07514.

Pye, J.M., 1988. Impact of ozone on the growth and yield of trees: a review. J. Environ. Qual. 17, 347–360.

Ramanathan, V., Feng, Y., 2008. On avoiding dangerous anthropogenic interference with the climate system: formidable challenges ahead. Proc. Natl. Acad. Sci. U.S.A. 105, 14245–14250.

Reich, P.B., Amundson, R.G., 1985. Ambient levels of ozone reduce net photosynthesis in tree and crop species. Science 230, 566–570.

Rieder, H.E., Frossard, L., Ribatet, M., Staehelin, J., Maeder, J.A., DiRocco, S., Davison, A.C., Peter, T., Weihs, P., Holawe, F., 2013. On the relationship between total ozone and atmospheric dynamics and chemistry at mid-latitudes: part 2. The effects of the El Nino/Southern Oscillation, volcanic eruptions and contributions of atmospheric dynamics and chemistry to long-term total ozone changes. Atmos. Chem. Phys. 13, 165–179.

Rustad, L.E., Campbell, J.L., Cox, R.M., DeBlois, M., Dukes, J.S., Huntington, T.J., Magill, A.H., Mohan, J.E., Pontius, J., Richardson, A.D., Rodenhouse, N.L., Watson, M.R., Willard, N., 2009. NE Forests 2100: a synthesis of climate change impacts on forests of the Northeastern US and Eastern Canada. Can. J. For. Res. 39, iii–iv.

Sitch, S., Cox, P.M., Collins, W.J., Huntingford, C., 2007. Indirect radiative forcing of climate change through ozone effects on the land-carbon sink. Nature 448, 791–794.

Solomon, S., Plattner, G.K., Knutti, R., Friedlingstein, P., 2009. Irreversible climate change due to carbon dioxide emissions. Proc. Natl. Acad. Sci. U.S.A. 106, 1704–1709.

Stein, S., Geller, R.J., 2012. Communicating uncertainties in natural hazard forecasts. EOS 93, 361–362.

Sun, G., McLaughlin, S.B., Porter, J.H., Uddling, J., Mulholland, P.J., Adams, M.B., Pederson, N., 2012. Interactive influences of ozone and climate on streamflow of forested watersheds. Global Chang. Biol. 18, 3395–3409.

Sverdrup, H., Warfvinge, P., 1993. Calculating field weathering rates using a mechanistic geochemical model PROFILE. Appl. Geochem. 8, 273–283.

Templer, P.H., Pinder, R.W., Goodale, C.L., 2012. Effects of nitrogen deposition on greenhouse-gas fluxes for forests and grasslands of North America. Front. Ecol. Environ. 10, 547–553.

Tkacz, B., Moody, B., Castillo, J.V., Fenn, M.E., 2008. Forest health condition in North America. Environ. Pollut. 155, 409–425.

Unger, N., Pan, J.L., 2012. New directions: enduring ozone. Atmos. Environ. 55, 456–458.

US EPA, 2008. Integrated Science Assessment (ISA) for Oxides of Nitrogen and Sulfur—Environmental Criteria, final report, Washington, DC.

Vingarzan, R., 2004. A review of surface ozone background levels and trends. Atmos. Environ. 38, 3431–3442.

Wang, H., Jacob, D.J., Le Sager, P., Streets, D.G., Park, R.J., Gilliland, A.B., van Donkelaar, A., 2009. Surface ozone background in the United States: Canadian and Mexican influences. Atmos. Environ. 43, 1310–1319.

Washington, W.M., et al., 2000. Parallel Climate Model (PCM) control and transient simulations. Climate Dyn. 16 (10), 755–774. http://dx.doi.org/10.1007/s003820000079.

Wittig, V.E., Ainsworth, E.A., Long, S.P., 2007. To what extent do current and projected increases in surface ozone affects photosynthesis and stomatal conductance in trees? A meta-analytic review of the last 3 decades of experiments. Plant Cell Environ. 30, 1150–1162.

Wu, W., Driscoll, C.T., 2010. Impact of climate change on three-dimensional dynamic critical load functions. Environ. Sci. Technol. 44, 720–726.

Yuan, F.-M., Meixner, T., Fenn, M.E., Simunek, J., 2011. Impact of transit soil water simulation to estimated nitrogen leaching and emission at high- and low-deposition forest sites in Southern California. J. Geophys. Res. 116, http://dx.doi.org/10.1029/2011JG001644, G03040.

Zhang, X., Zwiers, F.W., Hegerl, G.C., Lambert, F.H., Gillett, N.P., Solomon, S., Stott, P.A., Nozawa, T., 2007. Detection of human influence on twentieth-century precipitation trends. Nature 448, 461–465.

Zhang, L., Jacob, D.J., Downey, N.V., Wood, D.A., Blewitt, D., Carouge, C.C., van Donkelaar, A., Jones, D.B.A., Murray, L.T., Wang, Y., 2011. Improved estimate of the policy-relevant background ozone in the United States using the GEOS-Chem global model with 1/2o x 2/3 horizontal resolution over North America. Atmos. Environ. 45, 6769–6776.